Studies on the Interplay between the Network Architecture and the Dynamical Criticality of the Brain

by

Kamyar Mohammadzadeh Roudakian

A Dissertation Submitted to the
Graduate School of Sciences and Engineering
in Partial Fulfillment of the Requirements for
the Degree of

Master of Science

in

Physics

9 May, 2024

Studies on the Interplay between the Network Architecture and the Dynamical Criticality of the Brain

Koç University

Graduate School of Sciences and Engineering

This is to certify that I have examined this copy of a master's thesis by

Kamyar Mohammadzadeh Roudakian

and have found that it is complete and satisfactory in all respects,
and that any and all revisions required by the final
examining committee have been made.

Committee Members:

_____

Assoc. Prof. Alkan Kabakçıoğlu (Advisor)

_____

Assoc. Prof. Menderes Işkın

_____

Asst. Prof. Neşe Aral

Date: _____

[To my grandmother, whose wisdom, love, and guidance have been a constant source of inspiration, and to my family, for their unwavering support and encouragement throughout my journey.]

ABSTRACT

Studies on the Interplay between the Network Architecture and the Dynamical Criticality of the Brain
Kamyar Mohammadzadeh Roudakian
Master of Science in Physics
9 May, 2024

The critical brain hypothesis is a theory in neuroscience that suggests that the brain operates near a critical point between stability and instability where quantities like information flow diverge. In this thesis, we explore the brain's functional robustness and how its critical behavior relies on the structural components of its network. We demonstrate that the critical behavior of the brain network is linked to its Laplacian spectrum. Furthermore, we show that the brain's architecture can be reconstructed using Laplacian-based information maximization rewiring steps, referred to as adaptive rewiring. Through adaptive rewirings, the brain network undergoes an entropic phase transition, which allows it to maximize its functional abilities. These findings suggest a profound connection between the brain's structural determinants and its operational efficacy at the edge of criticality."

ÖZETÇE

Beynin Ağ Mimarisi ve Dinamik Kritikliği Arasındaki Etkileşim Üzerine Çalışmalarşlığı

Kamyar Mohammadzadeh Roudakian

Fizik, Yüksek Lisans

9 Mayis 2024

Kritik beyin hipotezi, nörobilimde bir teoridir ve beynin kararlılık ve kararsızlık arasındaki kritik noktada işlediğini öne sürer; burada bilgi akışı gibi miktarlar ayrışır. Bu tezde, beynin işlevsel dayanıklılığını ve kritik davranışının ağının yapısal bileşenlerine bağlı olduğunu araştırıyoruz. Beyin ağının kritik davranışının, Laplacian spektrumuyla ilişkilendirildiğini gösteriyoruz. Dahası, beyin mimarisinin, Laplacian temelli bilgiyi en fazla artıran yeniden bağlama adı verilen adaptif yeniden bağlama adımları kullanılarak yeniden oluşturulabileceğini gösteriyoruz. Adaptif yeniden bağlamalar aracılığıyla, beyin ağı entropik bir faz geçişine girer ve işlevsel yeteneklerini maksimize etmesine izin verir. Bu bulgular, beynin yapısal belirleyicileri ile kritiklik kenarındaki işlevsel etkinliği arasında derin bir bağlantı önermektedir.

ACKNOWLEDGMENTS

I would like to express my deepest gratitude to my dear advisor, Assoc. Prof. Alkan Kabakcıoğlu, for his invaluable guidance, limitless support, and encouragement throughout the course of this research. His insights and expertise have been instrumental in shaping the direction and quality of this thesis.

I am also immensely grateful to committee members, Assoc. Prof. Menderes Iskin and Asst. Prof. Nese Aral, whose constructive feedback and suggestions have enhanced the rigor and clarity of my work.

Special thanks go to my family for their unwavering support and patience during this journey. Their encouragement and understanding have been a source of strength and motivation.

I would like to extend my appreciation to the faculty and staff of the Science Department at Koç University for providing an excellent academic environment.

Additionally, I would like to acknowledge the financial support provided by Koç University, which has enabled me to focus on my research without financial concerns.

Finally, I am grateful to all those who have directly or indirectly contributed to the completion of this thesis. Your support and encouragement have been vital in bringing this work to fruition.

Kamyar M Roudakian

May 2024

TABLE OF CONTENTS

LIST OF TABLES

LIST OF FIGURES

ABBREVIATIONS

Greenberg Hastings	GHl
Resting State Networks	RSN
PCA	Principal Component Analysis
MF	MF
RR	Random Rewiring
AR	Adaptive Rewiring

Chapter 1

INTRODUCTION

The applications of statistical physics, which traditionally focused on the inanimate matter like gases, have significantly expanded over the past decades, extending far beyond the traditional domains [Castellano et al., 2007, Helbing et al., 2007, Garcia-Algarra et al., 2013]. This growth is attributed to the realization that the principles and methods of statistical physics have proven to be remarkably adaptable to a much broader range of systems, spanning from social contexts to biological systems. Examples range from gene regulatory networks to stock market crashes, which have effectively been described through the lens of statistical physics.[Nykter et al., 2008, Diep and Desgranges, 2021] These systems, known as "Complex systems" , are often composed of a large number of interconnected elements resulting in high degrees of freedom, and their collective behavior gives rise to an emergent complex phenomena. Emergence is the hallmark of complex systems, where higher-level properties of the system such as phase transitions and criticality emerge from the collective interactions of simpler elements. These emergent properties are not predictable just from the understanding of the microscopic levels but arise from the nature of being more in number; famously stated by Anderson in his seminal paper [Anderson, 1972]:

> "More is different."

More Interestingly, the macroscopic behaviour of the emergent phenomena in various systems often share common properties which able us categorize them in certain universal classes. The macro-level observable are characterized by distinct features including criticality and spontaneous order that set them apart from more simple or linear systems. Criticality as one of the key signatures complex systems can be

manifested in two ways: first, when a system unexpectedly transitions from one state to a very different state, at a point known as a 'Tipping/Critical Point,' and second, when a system experiences wild fluctuations and is highly sensitive to small changes in behaviors, termed as a 'Continuous Critical Transition'. Moreover, criticality in complex systems highlights how small events can trigger larger ones due to subtle inter-dependencies between elements, resulting in stratified chaos and unpredictable behaviors on different scales. Heterogeneity in complex systems' structure has been found to extend criticality, emphasizing that real-world complex systems are not homogeneous, with different elements changing at varying rates, contributing to robustness and adaptability, ultimately influencing the system's critical dynamics[Author, 2024a, Author, 2024b, Author, 2024c, Author, 2024d].

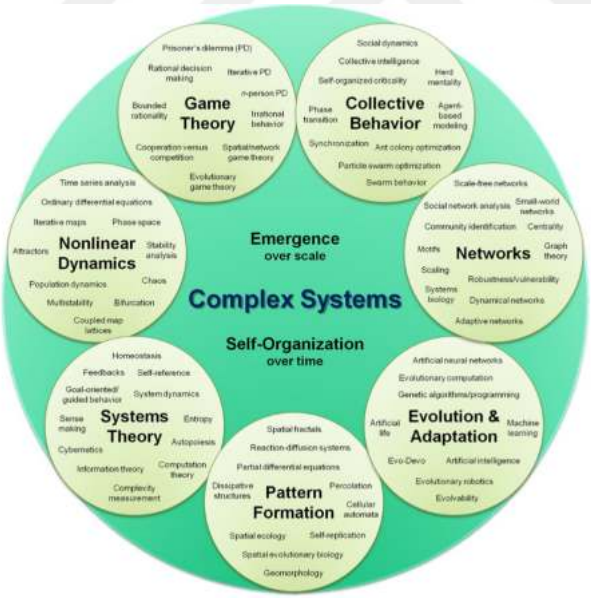

Figure 1.1: Complexity Science in one view. Picture from [lib,]

The human brain is a quintessential example of a complex system, exhibiting many of the key characteristics that define such systems. Understanding the brain as a complex system offers valuable insights into its functioning and the nature of its intelligence. Consciousness, memory, and cognition are not attributes of single

neurons but emerge from the dynamical interplay of neural circuits, meaning that individual processing systems at different functional scales are networked together , generating rich patterns of synaptic responses[Kaur et al., 2021]. In addition to emergence, the brain exhibits critical behaviour in its neurophysiological activity patterns. Brain critical hypothesis implies that the brain operates at a point of transition between orderly silent phase and chaotic disordered phase[Hesse and Gross, 2014]. A state believed to optimize its computational efficiency and responsiveness to environmental stimuli and enables the brain to balance stability and flexibility, while maintaining overall coherence.[Beggs, 2008, Shew and Plenz, 2013] Although the critical brain hypothesis had been proposed and explored theoretically in the 1990s mainly by Hertz and others [Herz and Hopfield, 1995, Stassinopoulos and Bak, 1995], the 2003 paper by Beggs and Plenz provided the first convincing experimental evidence supporting the criticality idea in brain[Beggs and Plenz, 2003]. They observed cascades of synchronized bursting activity that spread across the brain known as neuronal avalanches. Remarkably, they exhibit an inverse power-law scale-free distribution both in the spatial and temporal domains and the exponents of these power-law relationships align well with the theoretical predictions for a critical branching process. All of which posits that the collective dynamics of large neuronal networks in the brain operate close to the critical point of a phase transition[Beggs and Plenz, 2003, Shew et al., 2011, Cocchi et al., 2017].

Brain's synaptic connectivity rules as a structural basis to distribute the neural activity across brain regions. A departure from the typical topological arrangement may indicate a disruption or irregular operation of spatially dispersed brain regions that typically form a comprehensive network. This phenomenon has been evidenced in various neurological and psychiatric conditions such as schizophrenia[Moran et al., 2019] and Alzheimer's disease[Adriaanse et al., 2014]. Thus understanding brain connectivity as the centerpiece of brain functioning is crucial question in network's neuroscience and has been the matter of thousands of research projects in a diverse range of disciplines. Technological efforts in mapping brain connections has lead to advancements in our understanding of structural connections of human brain to get higher resolution of neural wiring of brain, called "Connectome"[Sporns, 2012].

In topological aspects connectome resembles a complex network by its high modularity and small world characteristic. The nested hierarchical structure of the brain supports the resilience and adaptability in different levels. This hierarchical organization not only contributes to the robustness and efficiency of the brain but also facilitates the information flow through neuronal pathways which at the end results in the emergence of complex cognitive functions.[Sporns, 2005]

The brain, as a real-world complex system, can indeed be effectively modeled by considering three key components: the static network of neurons representing structural order, the dynamic interactions within this network reflecting dynamical order, and the isolated dynamical behavior of individuals. This modeling approach allows for a comprehensive understanding of the brain's functioning at different levels of complexity. At the individual level, the brain exhibits isolated dynamical behavior that contributes to the overall functioning of the system through the dynamical interaction they have. These interactions involve the exchange of electrical and chemical signals between neurons, leading to patterns of activity that underlie cognitive processes.

In this thesis, the focus is on the interplay between the structural order, provided by the static neural connections, and the dynamical order, which emerges from the specific patterns of interaction facilitated by this structure. This interplay is crucial for understanding how the brain's physical architecture supports and shapes its dynamic processes, leading to its complex functionality. We investigate how the functionality of the brain is intricately dependent on its network structure, with properties like scale-free and small-world characteristics, modularity and the pattern of information flow. The functionality of the brain can be understood in various ways, reflecting the diverse and complex roles it plays in enabling and regulating numerous aspects of cognitive behavior. From the perspective of a physicist, especially one interested in complex systems, functionality of the brain might indeed be characterized in terms of its state of criticality. Studying the robustness of the critical state against attacks to neuronal connections sheds light on the the structure-function relation in brain.

In the course of this thesis, we will explore the question of the interplay between

network architecture and dynamical criticality in the brain in the following way:

Chapter 2 provides a theoretical framework for studying the structural organization of brain networks. This chapter lays the groundwork for understanding how the architecture of neural networks is influenced during rewiring processes.

Chapter 3 offers an overview of network neuroscience and the structure-function question, presenting a comprehensive picture of the human brain connectome. It examines the general measures and spectral properties of the human connectome, as well as its functional properties.

Chapter 4 reviews the concept of criticality, phase transitions, and the brain criticality hypothesis. This chapter includes a literature review on recent developments in brain criticality and introduces the Greenberg-Hastings cellular automaton, which serves as the main dynamical model for this thesis.

Chapter 5 investigates the uniqueness of the human brain's structural organization in the context of its criticality and information transfer. By perturbing the original network, we search for specific structural characteristics that may be responsible for the emergence of critical behavior. This chapter introduces a model for information diffusion in the brain network and proposes an evolutionary adaptive process, suggesting that the current human brain may result from this semi-Darwinian process. It demonstrates that through specific edge rewiring, brain criticality can be produced and maintained while preserving network structure.

Chapter 6 provides a comprehensive review of our findings and discusses potential future work.

Chapter 2

LAYING THE FOUNDATION: PRELIMINARIES IN GRAPH THEORY

Graph theory is the mathematical foundation on which the study of complex networks is developed. Over time, an extensive body of literature has emerged on complex networks, primarily originating from the physics community. The purpose of this chapter is to provide preliminary notions of graph theory, providing essential knowledge to comprehend and analyze complex networks. In this introductory chapter, the focus is on the undirected graphs as a special case of of directed graphs. For a more complete introduction see e.g. [Barabási, 2016, Newman, 2010]

2.1 Graphs

Graph is a mathematical structure providing a basis to represent pairwise interaction between objects; a network is a graph $G(V, E)$ consists of a set of N vertices (nodes) and a set of E of L edges (links) connecting through the adjacency relation. Two vertices v and u are adjacent if there exists an edge $e \in E$ that connects them. This is often denoted as $(u, v) \in E$ or equivalently $(v, u) \in E$ for undirected graphs. A network is called simple if nodes do not have self-interactions. In terms of graph representation, the adjacency relation can be expressed through an adjacency matrix.

2.1.1 The Adjacency Matrix

The adjacency matrix is a square matrix that represents a given finite graph. The elements of the matrix indicate whether pairs of vertices are adjacent or not in the graph.

In the adjacency matrix A of a graph G, the entry $A[i][j]$ is an attribute of the

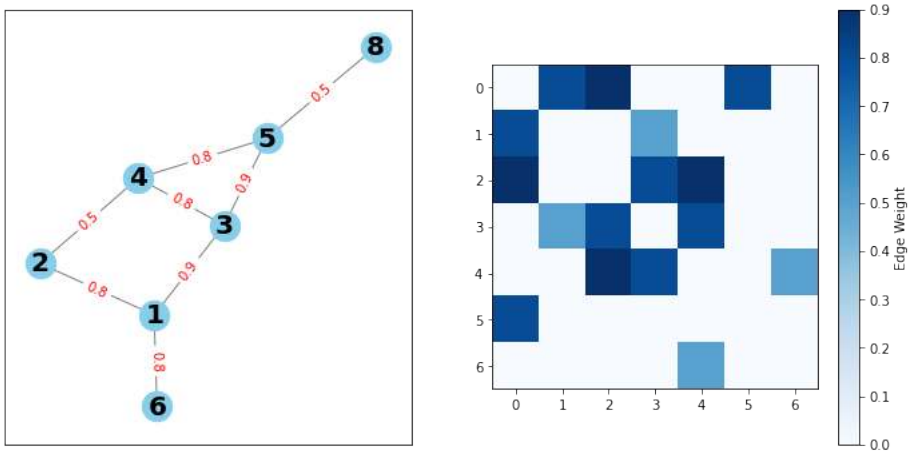

Figure 2.1: Human Connectome

edge between vertices i and j, which usually shows the strength of the link of two adjacent nodes, 1 in case of an unweighted, undirected graph. For an unweighted graph without loops, the diagonal elements of the matrix are all zero.

$$A_{ij} = \begin{cases} 1 & \text{if } i \text{ and } j \text{ are connected,} \\ 0 & \text{otherwise.} \end{cases} \tag{2.1}$$

The adjacency matrix is a powerful tool as it provides a compact representation of the graph, facilitating the analysis of the graph's properties.

2.1.2 Degrees

The degree of a vertex v in an undirected graph can be mathematically defined as follows

$$deg(v) = \sum_{u \in V} A[u][v].$$

Here, V is the set of all vertices in the graph, and A is the adjacency matrix of the graph. Thus, the sum of the entries in any row or column of the adjacency matrix gives the degree of the corresponding vertex. For weighted undirected networks this can be a measure of total strength of interaction.

2.1.3 Paths and Walks

A path is a sequence of connected non-repeated vertices. Mathematically, a path of length n from vertex v_0 to v_n is a sequence $P : (v_0, v_1, \ldots, v_n)$ such that $(v_i, v_{i+1}) \in E$ for $0 \leq i < n$, and all v_i are distinct.

A walk, on the other hand, is a sequence of vertices and edges in a graph such that each edge's end vertices are the preceding and following vertices in the sequence. Unlike a path, a walk can visit the same vertex multiple times.

In an undirected graph, a walk of length n from vertex v_0 to v_n is a sequence $W : (v_0, e_1, v_1, e_2, v_2, \ldots, e_n, v_n)$ such that edge e_i is incident with vertices v_{i-1} and v_i for $1 \leq i \leq n$. The length of the walk is the number of edges it uses, which may be less than the total number of vertices if some vertices are visited more than once.

2.2 Network measures

Network measures are quantitative measurements that are used to analyze and describe the structural properties and characteristics of complex networks, including the brain. In this section we will introduce the most important and relevant metrics which will give insights into the organization and behavior of the human brain networks.

2.2.1 Global Efficiency

The shortest path length L_{ij} is defined as the distance between pairs i and j along their shortest paths. The diameter of a network is the longest shortest path in the network. It is a measure of the maximum eccentricity of any node in the network. The average number of steps along the shortest paths for all possible pairs of network nodes is called "Average Path Length". Equivalently, the inverse of path length

$$E_{ij} = \frac{1}{L_{ij}} \tag{2.2}$$

is known as "Global Efficiency". The average efficiency of a network is defined as

$$E_{ave} = \sum_{i \neq j} E_{ij}, \tag{2.3}$$

which is in direct relationship with the efficiency of information or mass transport on a network.

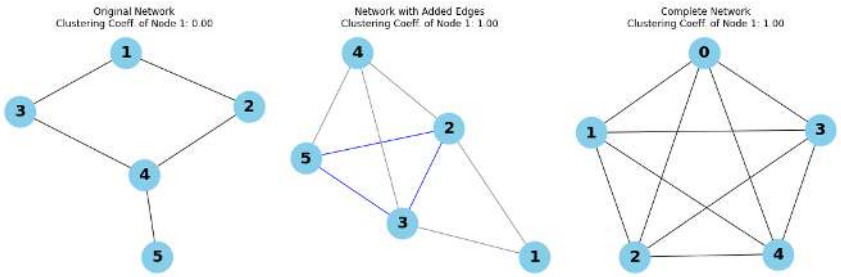

Figure 2.2: Shortest path

2.2.2 Connectivity

A graph is connected if we can find a path that span all vertices of the network, in another words there are no separate clusters.

2.2.3 Betweenness

The betweenness centrality of a node in a network measures the extent to which that node lies on the shortest paths between other pairs of nodes in the network. It quantifies a node's potential to control the flow of information or resources between other nodes and can be defined as

$$C_B(i) = \sum_{s \neq i \neq t} \frac{\sigma_{st}(i)}{\sigma_{st}}. \tag{2.4}$$

It calculates the fraction of shortest paths between all pairs of nodes in the network that pass through node i, and the sums these fractions for all pairs of nodes except when i is the source or target node.

2.2.4 Clustering Coefficient

The *clustering coefficient* of a vertex quantifies how close its neighbors are to being a clique (complete graph). It is a measure of local cohesiveness of a network that

quantifies the degree to which nodes in a graph tend to cluster together. For a given vertex, it is defined as follows. Let v be a given vertex, $N(v)$ be the set of neighbors of v, and $E(v)$ be the set of edges between the vertices in $N(v)$. The clustering coefficient $C(v)$ for a vertex v can be calculated using the formula

$$C(v) = \frac{2|E(v)|}{|N(v)|(|N(v)| - 1)}. \tag{2.5}$$

The *weighted clustering coefficient*, C_w, takes into account the weights of the edges forming these triplets and is defined as

$$C_w = \sum_{i=1}^{n} c_i^w,$$

where c_i^w measures the clustering coefficient for node i and is expressed as

$$c_i^w = \frac{1}{s_i(d_i - 1)} \sum_{j,h} \frac{w_{ij} + w_{ih}}{2} \alpha_{ij}\alpha_{ih}\alpha_{jh}.$$

Here, s_i represents the strength, d_i is the degree of node i, w_{ij} is the weight of the connection between nodes i and j, and α_{ij} is a binary index that equals 1 if $w_{ij} > 0$ and 0 otherwise. Equation (3) also applies to binary networks.

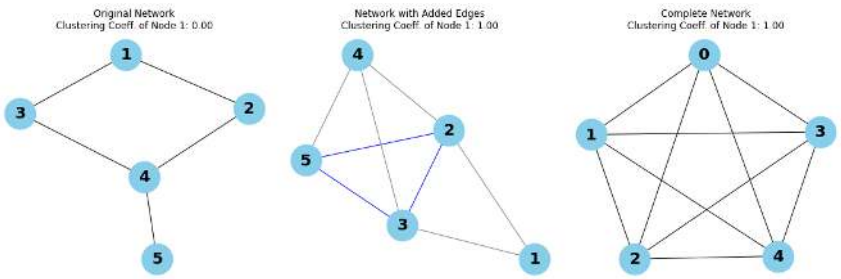

Figure 2.3: Human Connectome

2.2.5 Small-world Regime

A small-world network is type of graph in which most nodes are not directly connected to each other, but the neighbors of any given node are likely to be neighbors of each other and most nodes can be reached from every other by a small number

of hops or steps. In essence, a small-world network is characterized by a small average shortest path length, and a large clustering coefficient. To quantify small work regime of networks we take the normalized ratio of clustering coefficient to average shortest path length L.

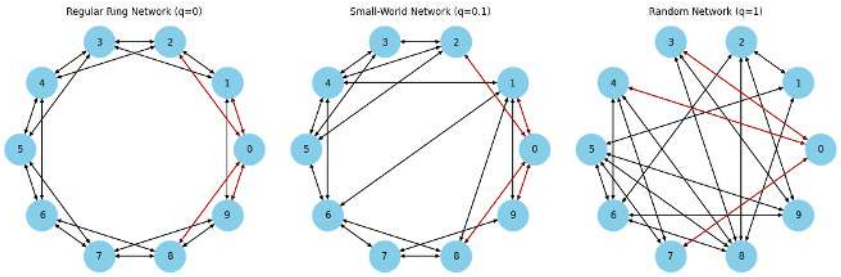

Figure 2.4: From Regular to Random: The transition from a regular ring network to a small-world and finally to a random network is shown

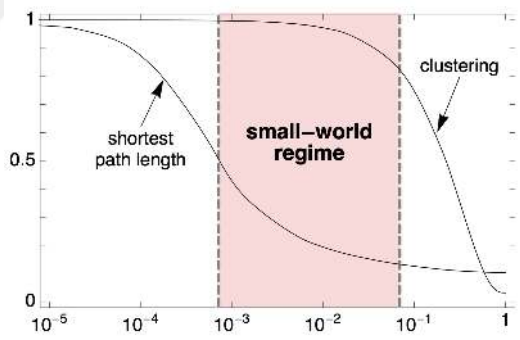

Figure 2.5: From Regular to Random: The transition from a regular ring network to a small-world and finally to a random network is shown.(Picture from []

2.2.6 Modularity

Modularity is a measure that quantifies the strength of division of a network into modules, also known as communities. Networks with high modularity have dense connections between the nodes within modules and sparse connections between nodes in different modules. Modularity is often used in optimization methods for

detecting community structure in networks.

$$Q = \frac{1}{2m} \sum_{ij} \left(A_{ij} - \frac{k_i k_j}{2m} \right) \delta(c_i, c_j), \tag{2.6}$$

where k_i and k_j are the degrees of node i and j, m is the number of edges in the network, c_i and c_j are the communities of node i and j, and $\delta(c_i, c_j)$ is 1 if nodes i and j are in the same community and 0 otherwise.

2.2.7 Assortativity

Assortativity in networks is a concept that refers to the tendency of nodes in a network to connect with others that are similar in some way. This characteristic is often seen in social networks where, for instance, individuals tend to form connections with others of the same age, race, or education level. In the context of network theory, assortativity usually refers to degree assortativity – a node's tendency to connect with others of similar degree.

A network is said to show assortative mixing if its nodes with high degree connect, on average, to others with high degree. Conversely, if high-degree nodes tend to connect to low-degree nodes, the network is said to show dis-assortative mixing.

is a number between -1 and 1 that measures the correlation between the degrees of all pairs of nodes connected by an edge. A positive assortativity coefficient indicates assortative mixing, while a negative coefficient indicates disassortative mixing.

The assortativity measure r can be calculated using the following formula

$$r = \frac{\sum_{ij} (A_{ij} - \frac{s_i s_j}{2m}) d_i d_j}{\sum_{ij} \left(s_i \delta_{ij} - \frac{s_i s_j}{2m} \right) d_i d_j}. \tag{2.7}$$

2.2.8 Rich Club Coefficient

The Rich Club Coefficient of a graph is a measure of the tendency of high-degree nodes to connect with each other more densely than would be expected in a random network. In other words, it quantifies the extent to which well-connected nodes are also well-connected among themselves, forming a "rich club".

Let N_k be the set of nodes in a graph that have a degree greater than k, and by E_k the number of edges that connect nodes in N_k. The rich-club coefficient $\Phi(k)$ for

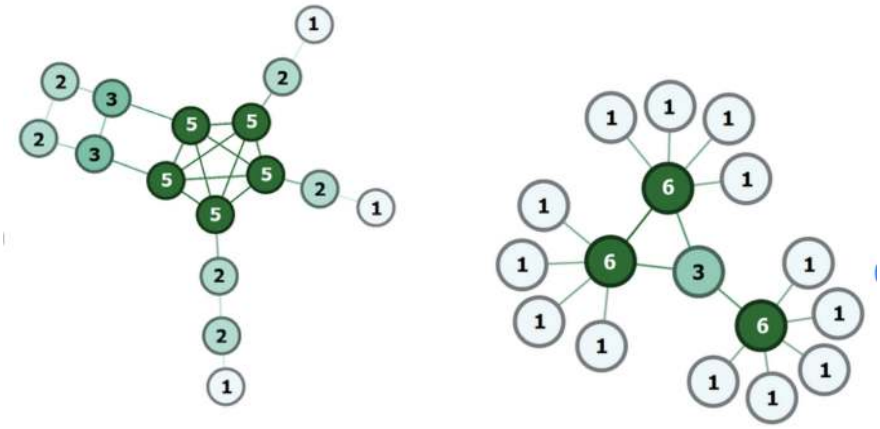

(a) (b)

Figure 2.6: (a) assortative network, (b) disassortative network

degree k is defined as

$$\Phi(k) = \frac{2 \cdot E_k}{|N_k| \cdot (|N_k| - 1)}.$$

Here, $|N_k|$ is the number of nodes in N_k. This coefficient represents the ratio of the number of edges E_k and the total number of possible edges between nodes in N_k.

2.3 Spectral Properties

In addition to real space characteristics which we discussed in the previous sections, there exist another group of measures derived from the spectrum of matrices associated with networks. It has been shown that the spectrum have a close relation with the many graph characteristics and can provide global measures for some network properties.

2.3.1 Adjacency Based Measures

spectral radius

The largest or the principal eigenvalue 1 of the adjacency matrix is called the spectral radius. The spectral radius of a network, often denoted as $\rho(A)$, is an important measure in graph theory. It is defined as the largest value of the eigenvalues of the

adjacency matrix. Mathematically, if the eigenvalues of a matrix A are $\lambda_1, \lambda_2, \ldots, \lambda_n$, then the spectral radius $\rho(A)$ is given by:

$$\rho(A) = \max\{|\lambda_1|, |\lambda_2|, \ldots, |\lambda_n|\}$$

The spectral radius is used to analyze the stability and dynamics of networks. In epidemiology, for example, it can predict the spread of a virus within a network, where a higher spectral radius might indicate a faster spread. REF [Wang et al., 2003]

Spectral gap

The difference between the largest and the second largest eigen- values of the adjacency matrix, denoted as $\lambda_1 - \lambda_2$, is called the spectral gap.

Natural connectivity

Natural connectivity is a vital metric in network science, capturing the robustness and structural integrity of a network. Unlike traditional measures it offers a more nuanced understanding of a network's resilience to perturbations. It is defined using the eigenvalues of the adjacency matrix of the network, which inherently incorporates both global and local structural properties.

Natural connectivity, denoted as λ_{nat} , is mathematically defined as:

$$\lambda_{\text{nat}} = \ln\left(\frac{1}{N}\sum_{i=1}^{N} e^{\lambda_i}\right)$$

where N is the size of the network, and λ_i are the eigenvalues of the adjacency matrix A. This definition leverages the exponential of the eigenvalues, making it sensitive to both the largest and the smallest eigenvalues, thus providing a more comprehensive measure of network connectivity. It can be interpreted as the average eigenvalue of the network's adjacency matrix in an exponential scale. This interpretation links it directly to the redundancy and fault tolerance of the network. A higher natural connectivity indicates a network that is more robust to random failures, as it implies a denser and more interconnected structure.

2.3.2 Graph Laplacian

The graph Laplacian, denoted as L, is a matrix derived from the adjacency matrix, A, of a graph. Mathematically, it is defined as:

$$L = D - A \tag{2.8}$$

where D is the diagonal matrix of node degrees, and A is the adjacency matrix.

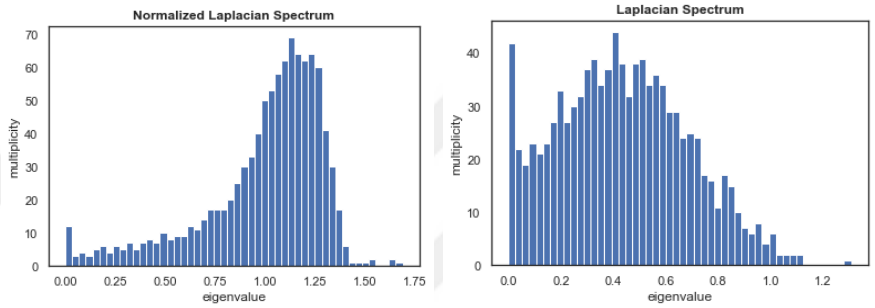

(a) (b)

Figure 2.7: Laplacian Spectrum

Algebraic connectivity

The second smallest, or the first non-zero, eigenvalue μ_2 of the Laplacian is called the algebraic connectivity. As the multiplicity of Laplacian eigenvalues equal to zero is related to the number of connected components, algebraic connectivity is equal to zero for disconnected graphs.

The figure 2.8 demonstrates several key properties of Laplacian spectra in neural networks. Firstly, it shows that the first eigenvalues are indicative of community structure within the network, with smaller first eigenvalues suggesting stronger community structures. Secondly, the figure illustrates how motif manipulations, such as the addition or duplication of motifs, result in distinct eigenvalues within the spectrum. These manipulations, when applied recursively, can produce eigenvalues with high multiplicities, leading to pronounced peaks in the Laplacian spectrum. Lastly, the figure highlights that the largest eigenvalue reflects the level of bipartiteness in

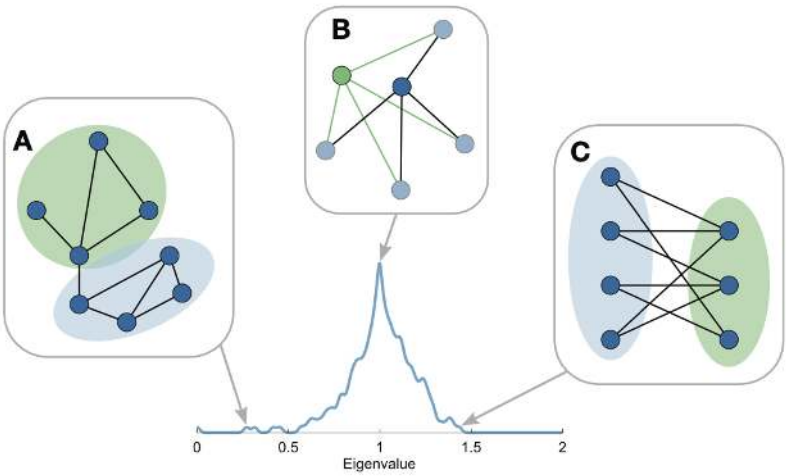

Figure 2.8: Topological properties of network as indicated by the Laplacian spectrum. From[de Lange et al., 2014]

the most bipartite subpart of the network, which is closely related to the presence of odd cyclic motifs. This relationship underscores the intricate interplay between network structure and the spectral properties of its Laplacian.

Chapter 3

CONNECTOMICS;

The intricate biological and cognitive processes within the human brain arise from the complex interplay of neural connections across various organizational levels. Describing these interactions within network theory framework proves remarkably fitting. Network neuroscience is a multidisciplinary field that integrates concepts from network science and neuroscience to study the brain's organization and function at various scales. It aims to comprehend connectivity patterns in genes, neurons and organisms, exploring how these patterns influence behavior.

Connectomics is a burgeoning field within network neuroscience that focuses on mapping the intricate connections of the brain and nervous system to understand how individual neurons are interconnected to form functional networks. It involves analyzing, and mapping the brain's neuro-physiological recordings using network models that represent brain areas as nodes and connections between them as edges. Utilizing tools from graph theory, algorithm development, statistical mechanics, and systems engineering we are able to shed light on our understanding of complex functions of brain.The scientific efforts to expand our knowledge of brain connectivity and enhance technological advancements in this field involve collaborations between various organizations and research infrastructures. Some examples of these research infrastructures include the Brain Initiative [of Health, 2014] , the Human Brain Project [Amunts et al., 2019] and the Human Connectome project [Van Essen et al., 2012]. In this chapter we will have a review on the concepts of structural and functional brain network, their difference and the relationship between them, then we will study the network theoretical and spectral measures of human connectome as a widely used structural brain network. At the end we will study the effect of edge perturbations through weight preserving double edge swaps.

3.1 Structural and functional networks

Structural and functional brain networks are two complementary aspects of how the brain is organized and operates. Structural networks refer to the physical connections between different brain regions. These connections are formed by bundles of nerve fibers known as axons, which transmit electrical impulses between neurons. Structural networks provide the anatomical framework that underlies brain function.

The structural connectome is typically generated using diffusion-weighted magnetic resonance imaging (DW-MRI) and tractography techniques. DW-MRI measures the diffusion of water molecules in brain tissue, which provides information about the orientation of the white matter fibers. Tractography algorithms then use this information to estimate the paths of white matter tracts connecting different brain regions. The structural connectome can be represented as a graph, where the brain regions are nodes and the white matter tracts are edges. This graph representation allows for the application of graph theory techniques to study the organization and properties of the brain's connectivity network.

An important example of structural brain networks is of C. elegans' which is the

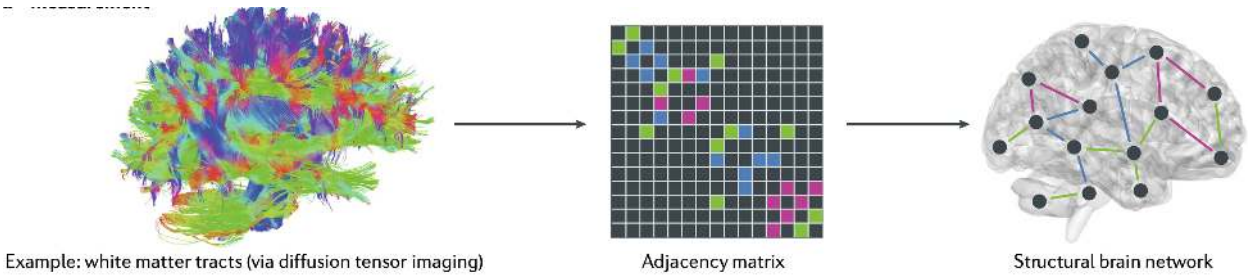

Figure 3.1: Structural networks extraction through DTI measurment. From[Lynn and Bassett, 2019]

first and last fully mapped neuronal connectivity which is extracted by electron microscopy techniques. The C. elegans nervous system consists of 302 neurons, are organized in a highly stereotypical and reproducible manner makes them an ideal

model organism for studying fundamental principles of neural function and behavior. Studying the structural brain network of C. elegans, uncovers fundamental principles of neural development, function, and plasticity that are applicable to more complex nervous systems, including those of humans.

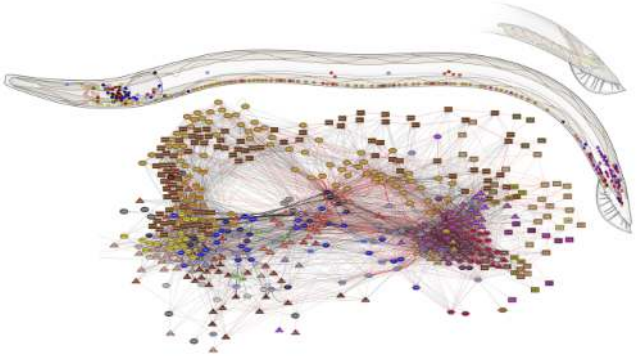

Figure 3.2: C.Elegans Structural network From[Cook et al., 2019]

In contrast, functional brain networks capture the patterns of correlated activity between brain regions, even in the absence of a direct structural connection. These networks are typically derived from functional neuroimaging data, such as fMRI, and reveal how different brain areas cooperate and communicate during rest or task performance.

Functional MRI (fMRI) captures activity within specific regions of the cortical volume by measuring blood oxygen level-dependent (BOLD) signals, which are closely linked to neuronal activity . When neuronal activity increases, there is a heightened demand for oxygen, prompting an increase in blood flow to areas of heightened neural activity. Oxygen is transported to neurons by hemoglobin in capillary red blood cells. Hemoglobin exhibits diamagnetic properties when oxygenated and paramagnetic properties when deoxygenated. This variance in magnetic characteristics results in subtle variations in the MR signal of blood based on oxygenation levels. As blood oxygenation levels fluctuate in response to neural activity, these distinctions can be utilized to detect brain activity.[Devlin et al., 2021, Bullmore and Sporns,

2009] While structural and functional networks are related, there is not a one-to-one

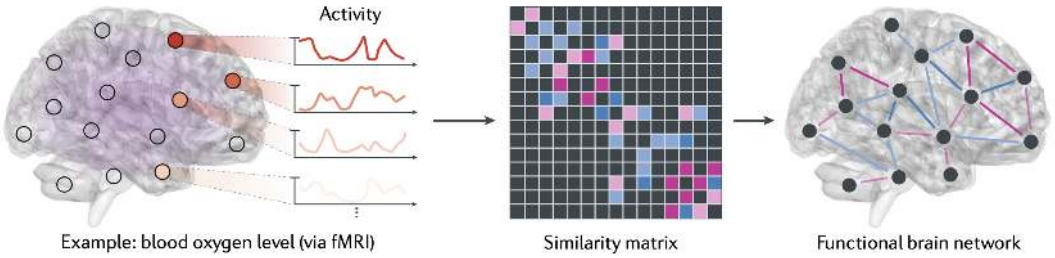

Figure 3.3: Steps to obtain structural network through DTI measurment From[Lynn and Bassett, 2019]

mapping between them. Structural connections provide the anatomical scaffolding for functional interactions, but functional networks can also emerge through indirect connections or synchronization of neural activity. Analyzing the coupling between structural and functional networks can provide insights into the neuro-biological basis of cognition and behavior.

3.2 Structure-Function Synergy

The brain's structural architecture and their intricate connectivity patterns, forms the substrate upon which dynamic functional processes unfold. The synergy between structure and function in brain networks is fundamental to understanding how the brain processes information, adapts to changes, and maintains its robust functionality.

Several important studies have provided substantial evidence on the relationship between structural and functional connectivity in the brain. Honey et al. (2009) demonstrated that structural connectivity could predict resting-state functional connectivity with significant accuracy, using diffusion tensor imaging (DTI) and functional MRI (fMRI). Their results indicated that the structural network's central hubs and modular organization are closely mirrored in the functional network, providing a foundational understanding of how anatomical connections influence brain dynamics[Honey et al., 2009] . Similarly, Hagmann et al. (2008) identified the

structural core of the human cerebral cortex and revealed that these core regions exhibit high functional connectivity, underscoring the critical role of structural hubs in coordinating large-scale brain activity [Hagmann et al., 2008].

Moreover, Goni et al. (2014) extended these findings by showing that analytic measures of structural network communication could predict resting-brain functional connectivity. Their work highlights the utility of graph-theoretical approaches in bridging the gap between structure and function, demonstrating that the efficiency of information transfer within structural networks is a strong predictor of functional interactions[Goni et al., 2014].

Studies combining both structural and functional networks in the same subjects have revealed a direct association between structural and functional connectivity in the human brain. Central hubs and clustered areas in structural networks are reflected at the functional level, and structural weights are significantly correlated with functional weights. However, even the best estimates place the correlation coefficient between structural and functional networks at around $R^2 \approx 0.5$, indicating that considerable variance in brain functional behavior is unexplained by a direct one-to-one correspondence with anatomical structure. A plausible explanation for this discordance between structure and function in the brain is the emergence of collective, higher-order interactions among neural elements that go beyond the geometric and locally clustered dependencies of graph-modeled structures. Functional interactions may result from indirect structural connections and are also driven by common inputs from sensory organs and the entire organism. Thus, brain functioning appears to be an emergent property of the human brain, resulting from complex interactions that cannot be fully captured by examining structural networks alone.

3.3 Human Brain Connectome

The connectome is a structural map of the physical connections within the brain, often described as its "wiring diagram." It describes the patterns of white matter tracts that connect different regions of the brain and provides insight into how information is transmitted and processed in the brain.

The structural connectome can be represented as a graph, where the brain regions are nodes and the white matter tracts are edges. This graph representation allows for the application of graph theory techniques to study the organization and properties of the brain's connectivity network. [?]

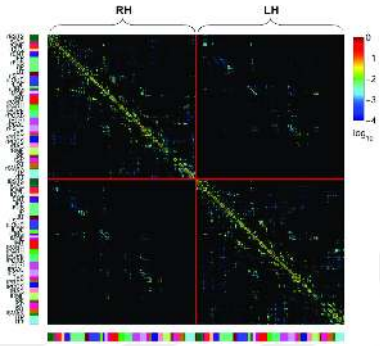

Figure 3.4: Human Connectome

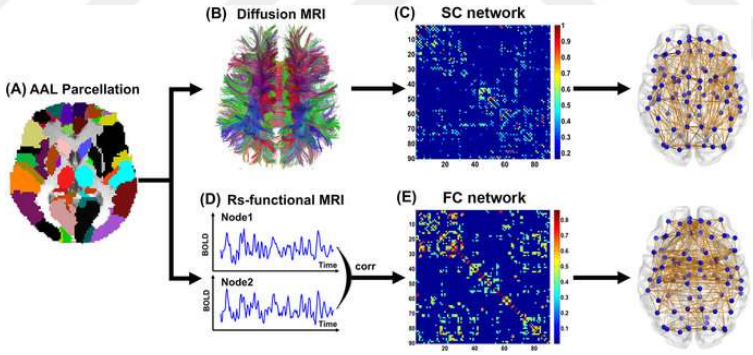

Figure 3.5: Deriving structural brain networks from Diffusion MRI and Functional brain networks from time series analysis

3.4 Connectome network architecture

In the analysis of the human brain's connectome, the structural properties outlined in the provided table offer significant insights into its complex network architecture. The connectome comprises 998 nodes and 17,865 edges, representing the neurons or brain regions and the synaptic connections between them, respectively. This

structure, with a network density of 0.036, reveals a sparse but efficient connectivity pattern characteristic of complex neural networks. Such sparsity ensures that the brain maintains a balance between metabolic cost and functional efficiency, essential for its sophisticated operations. The diameter of the network, recorded at 6, along with the existence of 6 separate components—the largest encompassing 898 nodes—underscores a high level of integration within the primary component, facilitating robust inter-regional communication across the brain's vast landscape.

The table further highlights an average clustering coefficient of 0.47, indicative of a moderate propensity for neurons or regions to form tightly-knit clusters. This clustering is crucial for creating functional modules within the brain, enabling specialized processing within distinct regions while ensuring cohesive global functionality through a short average shortest path length of 3.07. Such structural characteristics underscore the brain's 'small-world' nature, optimizing the balance between local specialization and global integration—a hallmark of neural efficiency. The degree assortativity value of 0.29 points to a network tendency wherein nodes preferentially attach to others with similar connectivity degrees, enhancing the network's resilience to disruptions. Additionally, the weighted mean degree and mean edge weight detail the network's connectivity strength, shedding light on the intricate balance between structural robustness and the nuanced dynamics of neural signal transmission. Collectively, these network properties not only reflect the underlying architectural principles guiding the brain's functional capabilities but also emphasize the sophisticated balance the brain achieves between complexity and efficiency, underscoring its remarkable capacity for processing and integrating information.

3.4.1 Degree distribution

The degree distribution P(k) is the probability of a node having k neighbors. The analysis of degree distribution in the human connectome is a critical aspect of understanding the complex network of the brain. The degree distribution analysis sheds light on how these connections are structured, revealing whether the brain operates as a regular network with a uniform distribution of connections or follows

Table 3.1: Connectome Network Properties Overview

Network Propperty	Value
Nodes	998
Edges	17865
Network Density	0.036
Diameter	6
Number of components	6
Largest Component Size	898
Average Clustering Coefficient	0.47
Average shortest path length	3.07
Global Efficiency	898
Degree Assortativity	0.29
Weighted Mean degree	0.44
Mean Edge Weight	0.00022

a scale-free pattern, where most nodes have few connections while a few hubs have many. This analysis is pivotal in identifying these hubs, which are integral for efficient information processing and network resilience. Furthermore, deviations in the typical degree distribution pattern can signal the presence of neurological disorders, offering a pathway to understanding diseases like Alzheimer's or Parkinson's, where such hubs may be impaired.[Naziroglu et al., 2015]

3.4.2 Edge weight distribution

Edge weight distribution analysis in the human connectome provides another layer of understanding, focusing on the strength or capacity of connections between brain regions. This aspect of network analysis is essential for deciphering the functional dynamics of the brain, revealing the intensity of interaction between different regions. It plays a crucial role in mapping functional connectivity, illustrating how various brain areas co-activate or co-suppress in response to different cognitive tasks

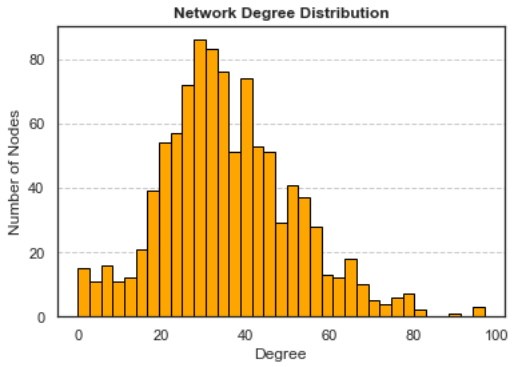

Figure 3.6: Degree Distribution

or environmental stimuli. Notably, changes in edge weight distributions can be indicative of different mental states or cognitive processes. In the context of neurological and psychological disorders, atypical patterns in edge weight distribution could serve as biomarkers, aiding in the diagnosis and understanding of conditions like schizophrenia or autism spectrum disorders.[Bullmore and Sporns, 2012, Fornito et al., 2015, Ecker et al., 2015]

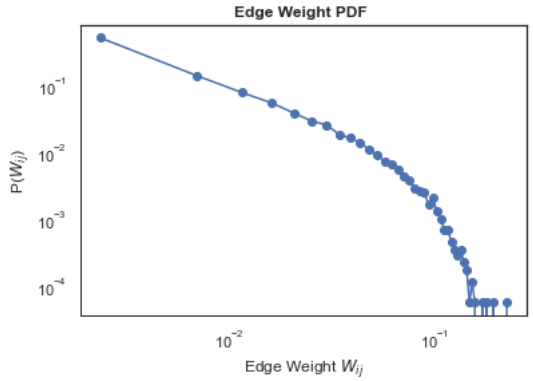

Figure 3.7: Brain Connectome's Edge weights distribution follow a power-law regime

3.4.3 Spectral Properties

The spectral properties of the brain connectome reveal crucial insights into the structural and functional integrity of the neural network. By examining the eigenvalues

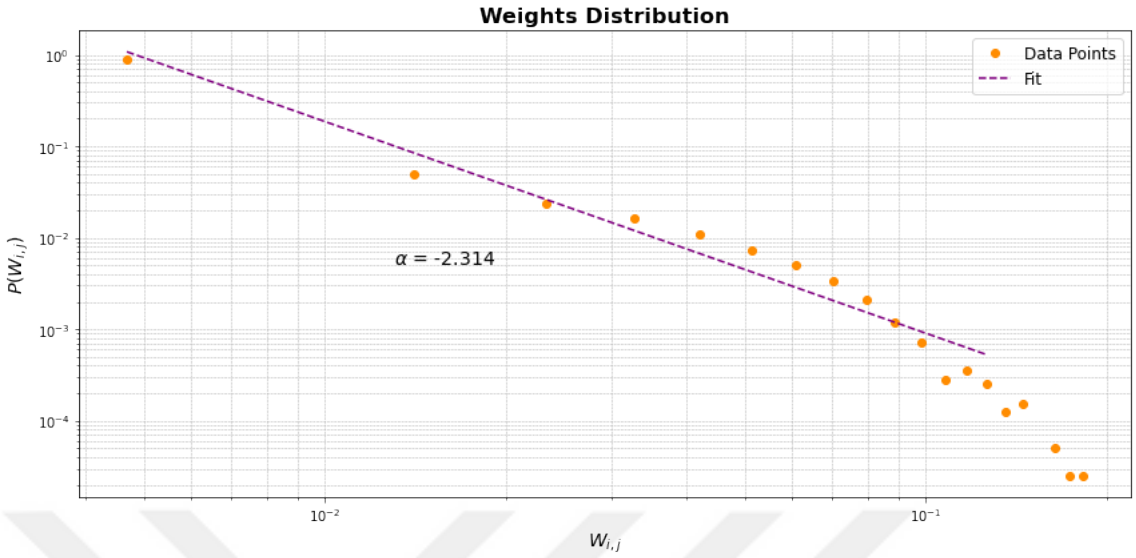

weights distribution power-law fit with an exponent $\alpha = -2.314$

of the adjacency and Laplacian matrices, we can infer significant characteristics about the brain's connectivity. The adjacency spectrum measures, including spectral radius, spectral gap, and natural connectivity, offer a window into the network's stability, robustness, and overall cohesion. For instance, a spectral radius of 0.671 indicates moderate stability within the network, while a small spectral gap of 0.053 suggests a certain fragility and sensitivity to perturbations. The low natural connectivity value of 0.01 further highlights the sparse and weakly connected components within the brain, indicating potential vulnerabilities in maintaining cohesive functional dynamics. These metrics collectively paint a picture of a network that, while moderately stable, is delicately balanced and susceptible to disruptions.

On the other hand, the Laplacian spectrum measures provide a different perspective, focusing on the flow and distribution of signals across the network. The extremely low algebraic connectivity of 0.0008 points to a nearly disconnected network, suggesting that the brain's ability to integrate information across different regions may be compromised. This is corroborated by the high effective resistance of 10980, indicating significant challenges for efficient signal transmission and communication within the network. Moreover, the absence of spanning trees underscores

the fragmented nature of the connectivity, highlighting the potential for isolated clusters that hinder unified brain function. Together, these spectral properties underscore the delicate balance of the brain's structural connectivity, revealing both its strengths and critical vulnerabilities in supporting complex neural processes.

Table 3.2: Adjacency Spectrum Measures Overview

Network Propperty	Value
Spectral radius	0.671
Spectral gap	0.053
Natural Connectivity	0.01

Table 3.3: Laplacian Spectrum Measures Overview

Network Property	Value
algebraic connectivity	0.0008
Effective Resistance	10980
spanning trees	0

3.5 Connectome Robustness Analysis

The robustness of networks refers to their ability to maintain functionality in the face of errors, failures, or attacks. Robustness measures of interest is highly dependent our definition of graph functioning and the way we perturb the original network. Here we focus on edge rewiring attacks which one can pres

3.5.1 Degree preserving Edge Rewiring

Degree-preserving edge rewiring serves as a well-defined method in the study of complex networks, allowing us to dissect the intricate relationships between network topology and dynamic processes. This technique maintains the edge weights

and degree distribution of nodes constant while altering the network's topology, enabling the exploration of network properties such as clustering, path lengths, and resilience without the confounding effects of changing degree sequences. This approach is invaluable for understanding how the arrangement of connections impacts processes like diffusion, robustness to failures, and synchronization across various networks, including brain systems. REF The basic procedure for degree-preserving edge rewiring involves the following steps: say (X,Y) and (W,Z), where X, Y, W, and Z are nodes in the network. These edges are chosen randomly, with the condition that they are distinct and do not share a vertex, to avoid self-loops and parallel edges. We Rewire the edges by swapping their endpoints to create two new edges (X,Z) and (Y,W), ensuring that these new edges do not already exist in the network and Repeat the process a sufficient number of times to achieve the desired level of mixing while constantly checking for and avoiding duplicate edges or self-loops. Al-

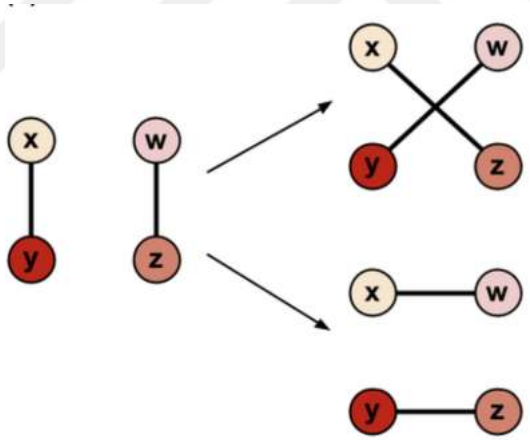

Figure 3.8: (a) The two degree-preserving double-edge swaps on a pair of edges (x, y), (w, z) results in either (x, y), (w, z) → (x, z), (w, y) or (x, y), (w, z) → (x, w), (y, z) as shown.

though the degree distribution remains unchanged, rewiring can significantly impact other network properties, such as clustering coefficients, average path length, and community structure.

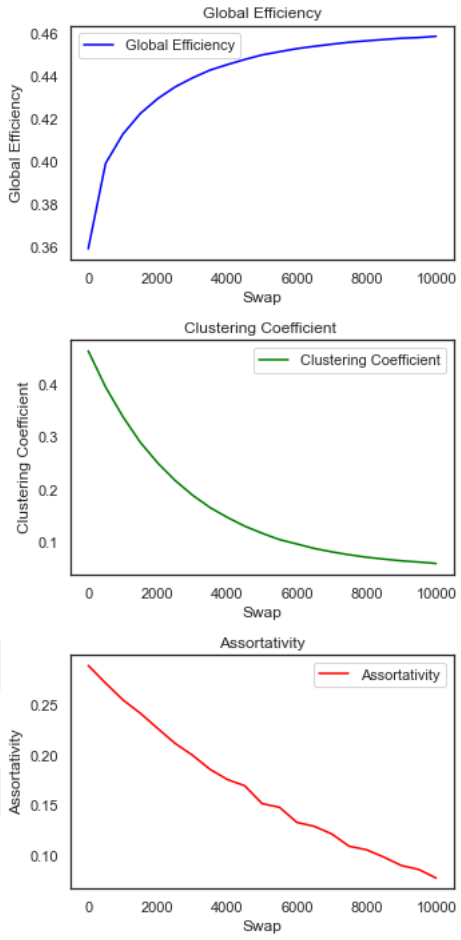

Figure 3.9: Connectivity network measures of brain connectome changes significantly in presence of random degree preserving edge rewiring

3.5.2 Monte-Carlo Method for Property Preserved Edge Rewiring

In the study of complex networks, the ability to explore and understand the impact of structural modifications is crucial. A Monte Carlo double-edge rewiring strategy offers a systematic approach to investigate network dynamics while preserving certain network measures. This method involves selectively rewiring edges in the network based on specific criteria, ensuring that key structural properties remain constant or are optimized. The essence of this approach is to balance the exploration of the network's configuration space with the preservation or enhancement of its functional characteristics.

To guide the decision-making process in this rewiring strategy, the Metropolis condition can be effectively applied. This condition is based on evaluating the change (ΔM) in a relevant network measure resulting from a proposed rewiring operation. If the change leads to an improvement or no impact on the targeted measure ($\Delta M \leq 0$), the rewiring is accepted. Conversely, if the change is detrimental ($\Delta M > 0$), the rewiring can still be accepted, but with a probability $P = \exp(-\Delta M/T)$, where T is a temperature-like parameter that controls the acceptance rate of less favorable changes. This probabilistic acceptance allows for a degree of exploration, enabling the network to escape local optima and potentially discover more advantageous configurations over time.

The implementation of this criterion requires generating a random number r within the range $[0, 1]$ and comparing it to P. If $r < P$, the rewiring is accepted; otherwise, it is rejected. This process not only ensures that the network can evolve towards optimizing specific measures but also introduces a controlled randomness that reflects real-world network dynamics. By adjusting the temperature parameter T, researchers can fine-tune the exploration-versus-optimization balance, facilitating a deeper understanding of how network structure influences its function and robustness.

Chapter 4

FROM NEURONS TO NETWORKS: COMPLEXITY IN THE BRAIN"

In this chapter, we bridge the gap between complex systems and neuroscience by approaching the brain as a complex system using tools and concepts from systems neuroscience. We examine the criticality hypothesis of the brain, which has strong foundations in the field of complex systems. Empirical evidence supporting this hypothesis will be highlighted, covering various aspects such as scaling properties and the phenomenon of neural avalanches. Several significant models, including the Ising Model, oscillatory models, and Integrate and Fire dynamics, will be introduced. Each model offers unique insights into the critical nature of complex systems and aids in understanding the underlying principles of such systems, including the human brain. A brief overview of each model will be provided, followed by an exploration of their potential connections. We then introduce the Greenberg-Hastings cellular automaton, which serves as the main framework of this thesis. Its potential impact on the structure-function relationship and the emergence of criticality in the human brain will be discussed.

4.1 Brain as a complex system

The human brain, an organ of extraordinary complexity, serves as the epicenter of thought, emotion, and behavior. It is often likened to a highly sophisticated computer, but its complexity far exceeds any man-made machine. It consists of approximately 86 billion neurons, each intricately connected to thousands of others, forming a complex network. This network is the foundation of all cognitive functions, from basic sensory processing to higher-order capabilities like reasoning, creativity, and consciousness.[Sporns, 2010] The brain's complexity is marked by several key char-

acteristics that distinguish it as a sophisticated system. One of these is non-linearity, where small inputs can lead to disproportionately large outputs, exemplified by how minor sensory inputs can trigger significant cognitive responses.[Steriade, 2001] This non-linearity is closely related to the concept of emergence, where complex behaviors and cognitive functions arise from the interactions of simpler neural processes. such as consciousness, memory, and decision-making, which are not confined to a single area but result from the dynamic interplay of various neural circuits.[Tononi and Edelman, 1998]

Understanding the brain as a complex system involves looking beyond the individual functions of neurons and considering the collective behavior and interactions of these elements. The emergent properties of the brain are key to this perspective. For instance, consciousness and self-awareness are not properties of individual neurons but rather arise from the complex interactions and organization of neuronal networks. The distinctiveness of the brain as a complex system lies not only in its large number of components. Rather, it is characterized by its adaptability, self-organization, and the criticality it exhibits. Self-organization is where patterns of neural activity and connectivity emerge from local interactions among neurons without a external controller, leading to organized behavior and cognition.[Kelso, 1995]

Adaptability and plasticity refers to the brain's remarkable ability to rewire itself in response to experiences and learning, a capability known as neuroplasticity. This adaptability is crucial for recovery from injuries, the acquisition of new skills, and adjustment to changing environments. [Pascual-Leone et al., 2005]These features collectively contribute to its complexity and functionality, setting it apart from simpler systems.

Each neuron, the fundamental working unit of the brain, operates through electrical and chemical signals. These neurons communicate via synapses, where neurotransmitters are released, allowing signals to pass from one neuron to another, creating a highly interconnected web of neural pathways. The dynamical activity patterns of neurons are indeed intricately linked with the dynamics of neural pathways, al-

though they operate on different time scales.[Buzsáki, 2006]
Examining the physiology of node dynamics (neuronal activity) and link dynamics (synaptic and network changes) in the brain is crucial for understanding how the brain processes information, learns, and adapts.

4.2 Neuronal Activity (Node Dynamics)

The action potential is a critical mechanism through which neurons communicate, characterized by rapid, transient changes in the neuron's membrane potential. This process is divided into three main phases: the quiescent phase, the excited phase (comprising depolarization and repolarization), and the refractory phases (absolute and relative). Each phase plays a specific role in the generation and propagation of the action potential.[Kandel et al., 2013]

4.2.1 Quiescent Phase (Resting State)

In the quiescent phase, the neuron is at rest with a stable membrane potential, typically around -70 mV. This resting membrane potential is maintained by the sodium-potassium pump, which actively transports sodium ions (Na) out of the cell and potassium ions (K) into the cell. This results in a negative charge inside the cell relative to the outside. During this phase, the membrane is more permeable to K ions than Na ions, and the voltage-gated sodium (Na) and potassium (K) channels are closed, keeping the neuron in a state of readiness for activation.[Bear et al., 2020]

4.2.2 Excited Phase

The excited phase, where the action potential occurs, involves significant changes in membrane potential and can be further divided into depolarization and repolarization sub-phases.

Depolarization:

A stimulus triggers depolarization, causing the membrane potential to become less

negative and approach zero. If this depolarization reaches a threshold (around -55 mV), voltage-gated Na channels open, allowing Na ions to rush into the cell due to the electrochemical gradient. This influx of Na causes the membrane potential to rise sharply, often peaking around +30 mV. This rapid rise in membrane potential constitutes the depolarization phase of the action potential.[Hodgkin and Huxley, 1952]

Repolarization:

Following the peak of depolarization, Na channels begin to inactivate, stopping further Na influx. Simultaneously, voltage-gated K channels open, allowing K ions to flow out of the cell. The efflux of K drives the membrane potential back toward the resting potential, making it more negative again. This phase of returning to a negative membrane potential is known as repolarization and is essential for resetting the neuron's membrane potential.[Hodgkin and Huxley, 1952]

4.2.3 Refractory Phase

The refractory periods ensure unidirectional propagation of the action potential and allow the neuron time to recover before firing again.

During the absolute refractory period, the neuron cannot initiate another action potential, regardless of the strength of the stimulus. This period overlaps with the depolarization and part of the repolarization phases when the Na channels are inactivated and incapable of reopening. Following the absolute refractory period, the neuron enters the relative refractory period. During this phase, a stronger-than-normal stimulus is required to elicit another action potential. This period coincides with the latter part of repolarization and extends into the hyperpolarization phase, where the membrane potential briefly becomes more negative than the resting potential due to continued K efflux. [Johnston and Wu, 1995]

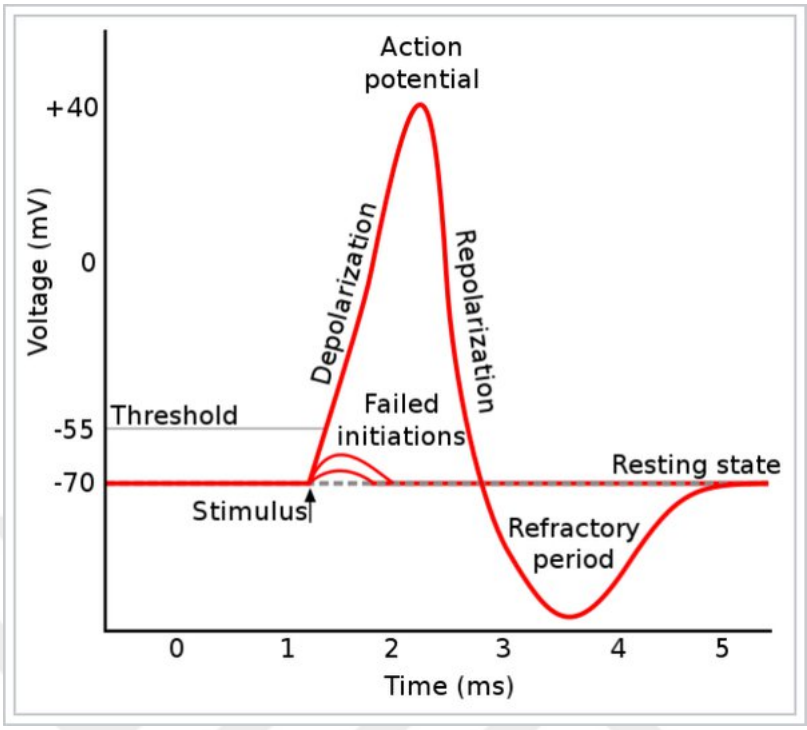

Figure 4.1: Diagram showing the phases of an action potential in relation to the membrane voltage over time. [From Wikipedia]

4.3 Synaptic and Network Changes (Link Dynamics)

The brain's remarkable ability to adapt and reorganize its neural connections in response to experiences and environmental changes is known as synaptic plasticity. Synaptic plasticity involves changes in the strength or efficacy of synapses, the connections between neurons, and is essential for learning, memory, and overall cognitive function. Four key mechanisms of synaptic plasticity are Hebbian dynamics, anti-Hebbian dynamics, spike timing-dependent plasticity (STDP), and homeostatic plasticity.

4.3.1 Hebbian - Anti-Hebbian Dynamics

Hebbian dynamics is the principle famously summarized by Donald Hebb in 1949: "Cells that fire together, wire together." According to Hebb, the synaptic connection between two neurons is strengthened when they are activated simultaneously.This

strengthening, known as long-term potentiation (LTP), enhances signal transmission between neurons, supporting learning and memory. LTP as a long-lasting increase in synaptic strength occurs when a presynaptic neuron repeatedly stimulates a postsynaptic neuron. This repeated stimulation leads to a sustained enhancement of signal transmission between the neurons, making the postsynaptic neuron more likely to fire in response to future stimuli.[Malenka and Bear, 2004]

Contrasting Hebbian dynamics, anti-Hebbian dynamics operate on the principle that "cells that fire apart, wire apart." This means that the synaptic connection between two neurons is weakened if one neuron is active while the other is not. This weakening, known as long-term depression (LTD), reduces synaptic efficacy and helps prune unnecessary connections, optimizing neural circuits.[Bear, 1995]

4.3.2 Homeostatic Plasticity

Homeostatic plasticity serves as a regulatory mechanism to maintain overall stability in the brain's activity levels. Unlike Hebbian and anti-Hebbian plasticity, which respond to specific patterns of activity, homeostatic plasticity adjusts the strength of all synapses in a neuron to stabilize its overall excitability. This type of plasticity ensures that neurons remain responsive to new inputs and prevents runaway excitation or inhibition that could disrupt neural network function[Turrigiano, 2012]. Homeostatic plasticity employs some mechanisms that ensure neurons operate within optimal ranges. Synaptic scaling adjusts the strength of all synapses on a neuron up or down to stabilize its firing rate. If a neuron becomes too active, synaptic scaling decreases the strength of its synapses, reducing excitability. Conversely, if a neuron becomes less active, synaptic scaling increases synaptic strength, enhancing excitability. This dynamic adjustment helps maintain a balance in neural activity, preventing runaway excitation or inhibition that could disrupt cognitive functions[Turrigiano and Nelson, 2004]. Complementing synaptic scaling, homeostatic intrinsic plasticity involves the regulation of voltage- and calcium-gated ion channels to fine-tune neuron excitability. By modulating the gain and firing thresh-

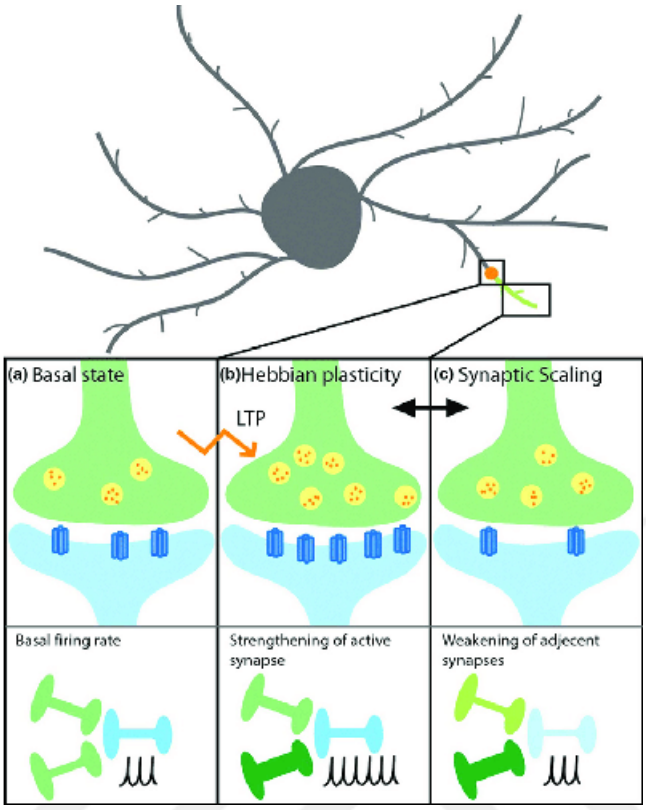

Figure 4.2: a)Basal state: Synapses use AMPARs(kind of acid receptors) to process stimuli, leading to a defined firing rate. b) Hebbian plasticity (LTP): Increased AMPAR insertion strengthens synapses, enhancing firing rate. c) Synaptic Scaling: Reduced AMPAR levels adjust synaptic strength to maintain optimal firing.From [Natascha Schaefer, 2017]

old of individual neurons, this process ensures that neurons can respond appropriately to varying levels of input, maintaining their activity within an optimal range. This intrinsic regulation is crucial for sustaining overall network stability and preventing the neurons[Marder and Prinz, 2003].

4.4 Self-Organized Criticality and Emergence

Phase transitions and critical phenomena are central themes in statistical physics. Materials, under varying conditions, undergo different phases. The universal nature of different classes of critical phenomena—highlighted by the fact that critical be-

haviors are largely independent of the microscopic features of a system—facilitates the application of criticality concepts, such as scaling laws, critical exponents, and percolation, beyond physical systems to include social and neural networks.
[Bak and Paczuski, 1995] Experimental evidence suggests that as systems approach a critical point, they begin to exhibit collective behaviors not present in their individual components. These emergent behaviors, from the alignment of spins in a ferromagnetic material to the cascading of neuronal avalanches, underscore the establishment of long-range spatio-temporal correlations among the system's components. Real-world examples of such emergence are plentiful, including the conscious awareness that emerges from neural networks in the brain and the flocking behavior observed in birds, demonstrating the broad applicability of criticality across different domains.
In many cases, reaching a system's critical point requires adjusting an external parameter, as exemplified by the Ising model, where temperature must be tuned to observe a phase transition. However, many systems achieve criticality without any external manipulation. The principle of self-organized criticality (SOC) is pivotal in understanding this aspect, positing that complex systems inherently progress toward a critical state without the necessity for external parameter adjustments. This concept is illustrated by well known phenomena the avalanches observed in a sandpile model, where the system naturally evolves to a critical state. In such a state, minor disturbances can trigger widespread, cascading effects. Self-organization describes the mechanism through which a system spontaneously increases its internal complexity, absent of direction from external forces.[Neumann, 1966]

4.5 Brain Critical Hypothesis

Critical phenomena in physics refer to the behavior of systems at or near critical points, where phase transitions occur, such as the transition in magnetic materials. At these points, systems exhibit scale invariance, meaning their properties more or less behave similar at all scales, and fluctuations occur over all possible sizes. Critical phenomena are characterized by power-law distributions and diverging correlation

lengths, highlighting the universal behavior across different physical systems[Stanley, 1971].

The hypothesis that the brain operates near a critical point originates from theoretical considerations and was further supported by early models of neural networks that employed systems such as spin glasses and cellular automata. The resemblance between the behaviors of these models and neural networks hinted at the potential for phase transitions within neural systems. At the phase transition points, networks display critical dynamics, balancing between chaotic and orderly states. Achieving and maintaining this delicate equilibrium in complex systems typically requires precise tuning, casting doubt on the brain's ability to naturally operate in such a state due to the improbability of such fine-tuning and a lack of empirical evidence. This skepticism persisted until the introduction of self-organized criticality (SOC) and pivotal experiments by Beggs and Plenz, which shifted the perspective.[Beggs and Plenz, 2003]

4.6 Some theoretical models of criticality

In this section, we will discuss three prominent theoretical models that elucidate the concept of criticality in brain dynamics. First, we will explore the Integrate and Fire model, which illustrates how neurons integrate signals and generate action potentials. Next, we will delve into the Ising model, adapted from statistical mechanics to study phase transitions and collective behavior in neural networks. Finally, we will examine the Oscillatory Kumamoto model, focusing on the role of oscillatory activity in maintaining critical states in the brain.

4.6.1 Integrate and Fire Model

he Integrate-and-Fire model offers a simplified framework for understanding neuronal dynamics. This model conceptualizes the neuron as an electrical circuit, integrating incoming synaptic potentials until a threshold is reached, upon which an action potential, or "spike", is generated, followed by a reset of the membrane poten-

tial. The elegance of this model lies in its abstraction of complex neuronal processes into a manageable mathematical formulation. Neuronal avalanches coming out of IF model are characterized by spontaneous bursts of activity that follow a power-law distribution, are indicative of critical dynamic in the brain.

[Gerstner et al., 2014] The mathematical formulation of the Integrate-and-Fire model is described by the following differential equation:

$$\frac{dV}{dt} = \frac{I_{\text{input}} - \frac{V}{R_m}}{C_m}$$

Here, $\frac{dV}{dt}$ represents the rate of change of the membrane potential V over time t, I_{input} is the input current, R_m denotes the membrane resistance, and C_m is the membrane capacitance. When V reaches a predetermined threshold value, the neuron fires an action potential, and V is subsequently reset to a baseline level, simulating the refractory period of actual neurons.

4.6.2 Oscillatory Dynamics

The Kuramoto model, developed in the late 1970s by Yoshiki Kuramoto, is a conceptual framework used to describe synchronization phenomena in systems of coupled oscillators. The model starts with a simple assumption: each oscillator in the system is characterized by its phase, and it interacts with other oscillators through a coupling that depends on the difference in their phases. By modeling neurons as oscillators with varying natural frequencies that interact with each other, the Kuramoto model captures the essence of neuronal synchronization, illustrating how collective neural dynamics emerge from the interactions within the brain's intricate networks. [Kuramoto and Kuramoto, 1984]

$$\frac{d\theta_i}{dt} = \omega_i + \frac{K}{N}\sum_{j=1}^{N}\sin\left(\theta_j - \theta_i\right) \tag{4.1}$$

Where θ_i represents the phase of i^{th} oscillator and $\omega_i$is its natural frequency, K is the coupling strength between the oscillators, and the summation term accounts for the sine of the phase differences, modeling the interaction between oscillators.

The Kuramoto model elegantly captures the transition from incoherence to synchronization as the coupling strength increases. At low coupling strengths, oscilla-

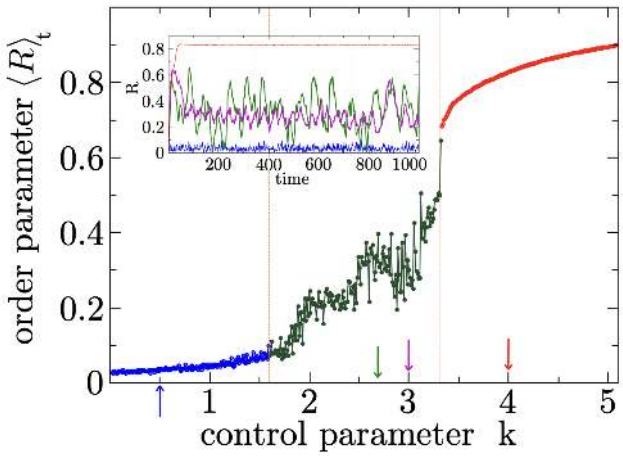

Figure 4.3: Time-averaged value of the order parameter for the noisy Kuramoto dynamics running upon the Human Connectome- Graph from [Villegas et al., 2014]

tors tend to oscillate independently according to their natural frequencies. As K increases, a critical threshold is reached where a significant fraction of oscillators starts to synchronize, exhibiting collective oscillations. (Figure 4.2)

4.6.3 Ising Model

The Ising model is a fundamental model in statistical physics and critical phenomena, introduced by Ernst Ising in 1925. It is originally conceived to describe ferromagnetism, has found intriguing applicability in the realm of neuroscience, particularly in modeling the complex dynamics of the brain. By simplifying the brain's network of neurons into a system of binary units—akin to the spins in the Ising model—this approach provides a powerful framework for exploring how individual neuronal interactions contribute to the emergent properties of brain activity. Each neuron is represented as being in one of two states, active or inactive, analogous to the spin-up or spin-down states in the Ising model, with the synaptic strengths between neurons mirroring the interaction terms between adjacent spins. This simplification allows to use the model to investigate the collective behavior of neurons, which explains how local synaptic interactions can give rise to global patterns of

neural activity, much as spins contribute to magnetic phenomena in physics. The Hamiltonian for the Ising model in the context of brain dynamics can be written as:

$$H = -\sum_{\langle i,j \rangle} J_{ij} s_i s_j - \sum_i h_i s_i, \tag{4.2}$$

where s_i represents the spin at site i, J is the interaction strength between neighboring spins comes from the adjacency matrix where, $\langle i, j \rangle$ indicates that the sum is over nearest neighbors only, and h_i is an external magnetic field applied to the system. At low temperatures, spins tend to align due to the interaction term, leading to a ferromagnetic phase. As the temperature increases, thermal fluctuations disrupt this alignment, leading to a paramagnetic phase. The transition between these two phases, characterized by a critical temperature T_c, is a second-order phase transition, which has been extensively studied in the context of the Ising model. [Amit et al., 1985]

4.7 Experimental evidence supporting brain criticality

Eguiluz et al. utilized fMRI data to map connections between different brain regions based on the strongest correlations observed through BOLD signals. Their findings revealed characteristics indicative of small-world and scale-free networks: a scale-independent distribution of connections and link probability relative to distance, a small characteristic path length similar to that of an equivalent random network, and a significantly higher clustering coefficient compared to equivalent random networks.[Tkačik et al., 2015]

Similarly, Fraiman's investigations into the dynamics of brain fluctuations at rest—without specific inputs or outputs—employed fMRI to compare correlation networks to simulations of the 2D Ising model at varying temperatures. The statistical properties at the critical temperature T_c made the two networks nearly indistinguishable, supporting the theory of criticality in brain function.

This section will further explore brain dynamics through the analysis of nLFP measurements by Beggs and Plenz. The observed avalanche shapes and branching

parameters are in line with predictions by Zapperi, indicating that at a critical branching probabilityp_c, avalanches exhibit power-law behaviors. Such observations are consistent with the phenomena of neuronal avalanches. The discussion will extend to examining the distribution of avalanche sizes and lifetimes, as well as the branching parameter, drawing on data from both nLFP and MEG studies, to underscore the brain's critical dynamics. [Chialvo, 2004, Levina et al., 2007, Zapperi et al., 1995, Levina et al., 2007]

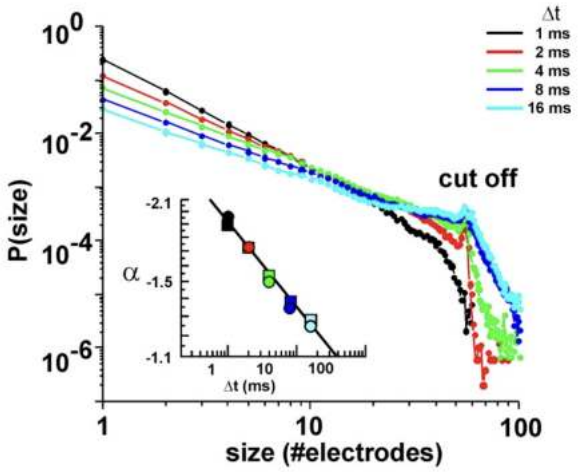

Figure 4.4: distribution of avalanches from nLFp experiments

4.7.1 Avalanche criticality

The cerebral cortex is predominantly made up of pyramidal neurons. These neurons are capable of receiving input signals through a complex web of dendrites from other neurons and, via their own axons, have the ability to excite neighboring neurons. Generally, the connections facilitated by these neurons are relatively weak, resulting in minimal stimulation for neuron activation. Thus, for a neuron to become activated, it requires stimulation from a collective of surrounding neurons. This implies that neurons need to operate in sync within an adequate and sensible time frame to prevent the network's activity from diminishing and to achieve synchronous neuronal firing. Synchronous activity within the brain has been observed as neuronal

oscillations and cascading activities within the cortex. In the following section will explore the concept of neuronal avalanches, examining the distribution of their sizes and duration, as well as the branching parameter, through the analysis of nLFP and MEG data. [Zare and Grigolini, 2013] [Stewart and Plenz, 2008][Beggs and Plenz, 2003][Gerstner et al., 2014] Experimental works done by Beggs[Beggs and Plenz, 2003] and colleagues marked a significant starting point for further experimental and theoretical cognitive neuroscience research that provides evidence of a critical brain state. I will further explore brain dynamics through the analysis of nLFP measurements by Beggs and Plenz.

nLFP The local field potentials are electrical signals that occur in the extracellular space surrounding neurons: These signals represent the synchronous activity of groups of neurons, which are measured using electrodes with high impedance. However, due to interference and potential decay over distance, their measurement capability is limited in scale.

Neuronal avalanches refers to the cascading sequence of neural activations within the brain,quantified through the graphical representation of neural activity over time. This phenomena is depicted by plotting the extent of neuronal activity as a function of time, where each avalanche represents a distinct episode of widespread neuronal firing. The 'lifetime' or duration of these avalanches is defined from the moment an avalanche is triggered to the point at which neural activity returns to baseline levels.

nLFP Experiment

The study sample will consist of organotypic cultures from somatosensory coronal slices of mice. The configuration of the electrode array can be seen in Figure [3].

By crossing a negative threshold the signals received from the micro electrodes, the synchronous activity of a group of neurons near the electrodes is identified (see Figure 4). Let's define the average branching parameter, denoted as σ, as follows.)

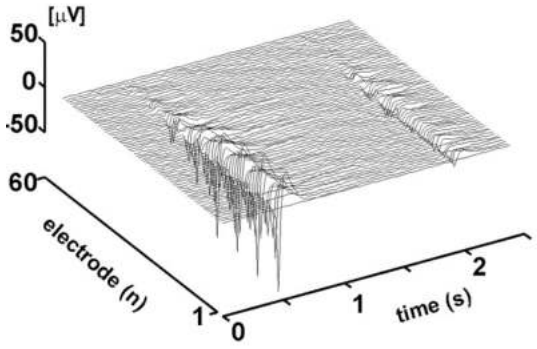

Figure 4.5: distribution of avalanches from nLFp experiments

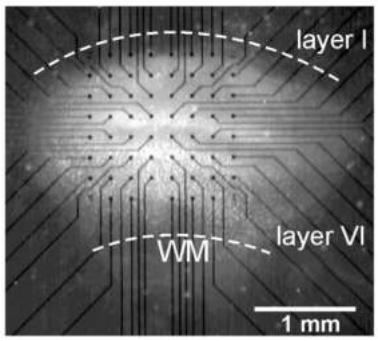

Figure 4.6: detecting nLFp's by thresholding

$$\sigma = \sum_{d=\cdot}^{n_{\max}} d \times p(d) \tag{4.3}$$

where d is the number of electrode descendants, $p(d)$ is the probability of observing d descendants, and $n$max is the maximal number of active electrodes. Although σ is defined as the branching parameter for a neuron (according to the branching parameter definition), in this case, it is equivalent to the number of descendants generated from a single neuron. We can define it for multiple neurons.

$$d = \text{round}\left(\frac{n_d}{n_a}\right) \tag{4.4}$$

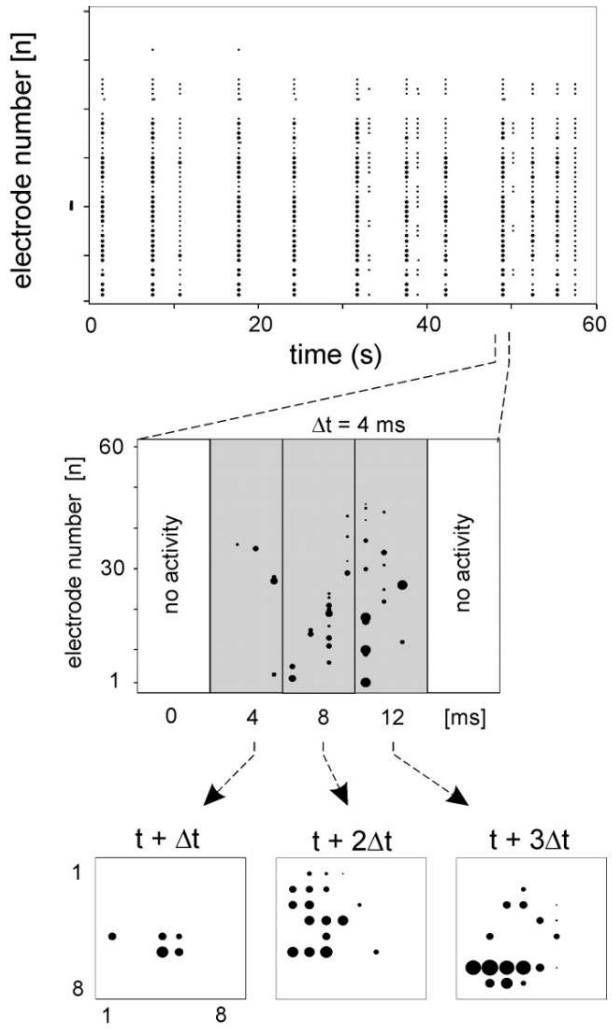

Figure 4.7: Definition of a neuronal avalanche

Where n_a is the number of active electrodes observed in the first time interval from the onset of the cascade, and similarly, n_d equals the number of active electrodes in the second time interval from the onset. Likewise, the probability of observing d descendants is approximated by

$$p(d) = \sum_{\text{avalanches}} \left(\frac{n_{\Sigma a|d}}{n_{\Sigma a}} \right) \left(\frac{n_{\max} - 1}{n_{\max} - n_a} \right) \tag{4.5}$$

where $n_{\Sigma a|d}$ was the total number of electrode ancestors in all avalanches when n_d descendants were observed, $n_{\Sigma a}$ was the total number of ancestors observed in all

avalanches, and

$$\left(\frac{n_{\max}-1}{n_{\max}-n_a}\right) \tag{4.6}$$

was a factor that provided an approximate correction for the reduced number of electrodes available in the next time bin because of refractoriness. By definition, we

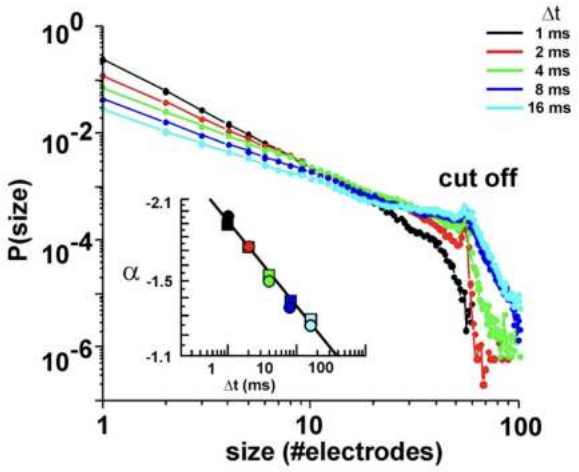

Figure 4.8: statistics of avalanches for different time differences

consider the size of avalanches to be equal to the number of electrodes that have crossed the threshold. As we can observe, the slope of the avalanche statistics is dependent on the chosen time interval. Choosing slope $\alpha = 1.5$ as a suitable slope can be justified by several observations: Firstly, the slope 1.5 is the point where differences emerge between various threshold ranges in the collected data. Secondly, because neuronal activity propagates at a limited speed, the time between calculating the activity of electrodes increases with the distance between the electrodes, while we know that the true slope of the power law must remain independent of such scaling. To address this issue, let's remove some internal electrodes with increasing time intervals, while keeping the array's dimensions constant. As can be seen from figure 5, In the constant ratio $\frac{\Delta d}{\Delta t}$ where Δd is the distance between electrodes and Δt is the time difference of event recording, a slope of 1.5 occurs. In general, this ratio can provide an approximate measure of the speed of neuronal activity propagation. Thirdly, the number of electrodes in which the resulting graph becomes cut

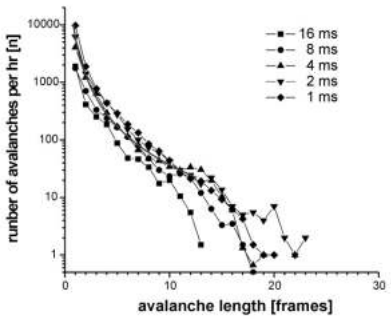

Figure 4.9: statistics of avalanches for different time differences

should be considered, taking into account the limited size of the electrodes and the constraints imposed in measurement. In the slope of 1.5, by halving the consecutive number of electrodes , it's observed that the cutoff point is independent of the measurement constraint imposed. Eventually, by increasing the distance between arrays according to Equation , we can observe the scale-free behavior following the power law. Additionally, the lifespan of avalanches (denoted as τ) can also serve as an

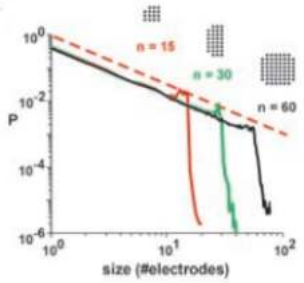

Figure 4.10: The cutoff determined by the number of electrodes

effective parameter in the dynamics of the system, providing valuable information. Theory and simulations have predicted that the distribution of lifetimes exhibits power-law behavior. We can observe scale-free behavior following the power law with exponent $\alpha = -2$. In conclusion, experiments done by Beggs et.al, showed that the distribution of neural avalanches, when analyzed in terms of their duration and the spatial extent of involved neural tissue, typically exhibits a power-law

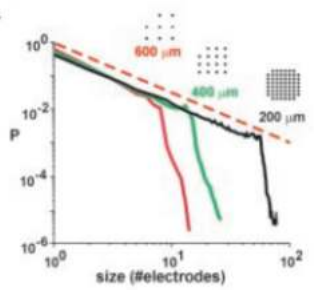

Figure 4.11: Increasing the distance between electrodes according to δt

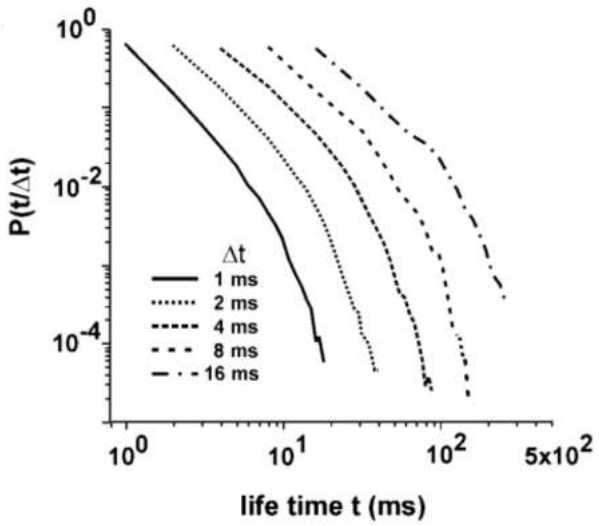

Figure 4.12: Increasing the distance between electrodes according to δt

distribution. This pattern of distribution is indicative of critical state dynamics supporting earlier theoretical works on brain's dynamical state.

4.7.2 Theromodynamic Criticality

Empirical studies have provided compelling evidence that the brain operates near critical points, a concept derived from statistical mechanics. One notable study by Tkacik et al. (2015) applied a thermodynamic framework to the activity of retinal ganglion cells. By defining a Boltzmann-like distribution for neural states, the researchers derived thermodynamic quantities such as heat capacity and observed

that it peaked near critical points. This peak indicates a divergence, suggesting that the neural network is highly sensitive and capable of large-scale reconfigurations in response to minimal external inputs. Such findings imply that the brain can dynamically adjust its functional connectivity, optimizing information processing and adaptability to environmental changes. The applicability of this framework to real biological systems highlights its potential for understanding the brain's complex dynamics [Tkačik et al., 2015].

Further supporting this notion, studies using functional MRI (fMRI) and magnetoencephalography (MEG) have observed power-law scaling in brain activity, indicative of critical dynamics. Kitzbichler et al. (2009) demonstrated that large-scale brain dynamics exhibit long-range temporal correlations consistent with critical states. By analyzing the temporal dynamics of functional connectivity, they found that the brain's susceptibility—its responsiveness to external perturbations—peaks near critical points. This peak in susceptibility aligns with theoretical predictions and suggests that the brain operates in a critical regime to balance stability and flexibility, essential for complex cognitive functions and adaptive behavior [Kitzbichler et al., 2009].

4.7.3 Criticality in Cortical Oscillations

Cortical oscillations exhibit critical behavior, characterized by power-law distributions in their power spectra. Freeman et.al analyzed electrocorticogram (ECoG) recordings and identified scale-free dynamics indicative of critical states. They observed that these oscillations, across various frequencies, display long-range temporal correlations and fractal-like patterns. This suggests that the brain operates near a critical point, facilitating efficient information integration and coordination of neural activity across different brain regions[Freeman et al., 2000].

4.7.4 bifurcation criticality

When a dynamical system transitions from one regime to another, such as from order to chaos, it undergoes a bifurcation. The point of transition is known as

the critical point. Bifurcations, including the transition from asynchronous to synchronous states, are crucial for understanding brain dynamics and computation. These critical transitions can co-occur with avalanche criticality during continuous phase transitions. However, Kanders et al. (2020) proposed that these two types of criticality might not always co-occur and should be considered distinct phenomena [Cocchi et al., 2017, Muñoz, 2018]\[Izhikevich2007 Kanders2020].

Research on epilepsy provides compelling evidence for bifurcation criticality. During seizures, the brain transitions from a normal state to a highly synchronized state. Studies using EEG recordings have shown that these transitions can be described by bifurcation theory, where the critical point corresponds to the onset of the seizure \[Jirsa2014]. Also research on the auditory cortex of gerbils have demonstrated bifurcation-like transitions in response to varying sound stimuli. By gradually increasing the amplitude of the auditory input, researchers observed a transition from a non-synchronized to a synchronized firing state among neurons, consistent with bifurcation criticality[Hahn2010] .

4.8 Greenberg-Hastings Dynamics

Among various brain models, the Greenberg-Hastings (GH) cellular automaton stands out as a particularly insightful tool for dissecting the dynamics of criticality in the brain. Initially developed to model excitable media, and later on introduced by Haimovici and collaborators to model neural activity. GH model's simplicity, coupled with its ability to produce rich dynamical behaviors, makes it an ideal candidate for exploring the principles of criticality.

The G-H model operates on a network where each cell can exist in one of three states: quiescent, excited, or refractory. The transition between these states is governed by straightforward rules that mimic the firing and recovery phases of neurons.

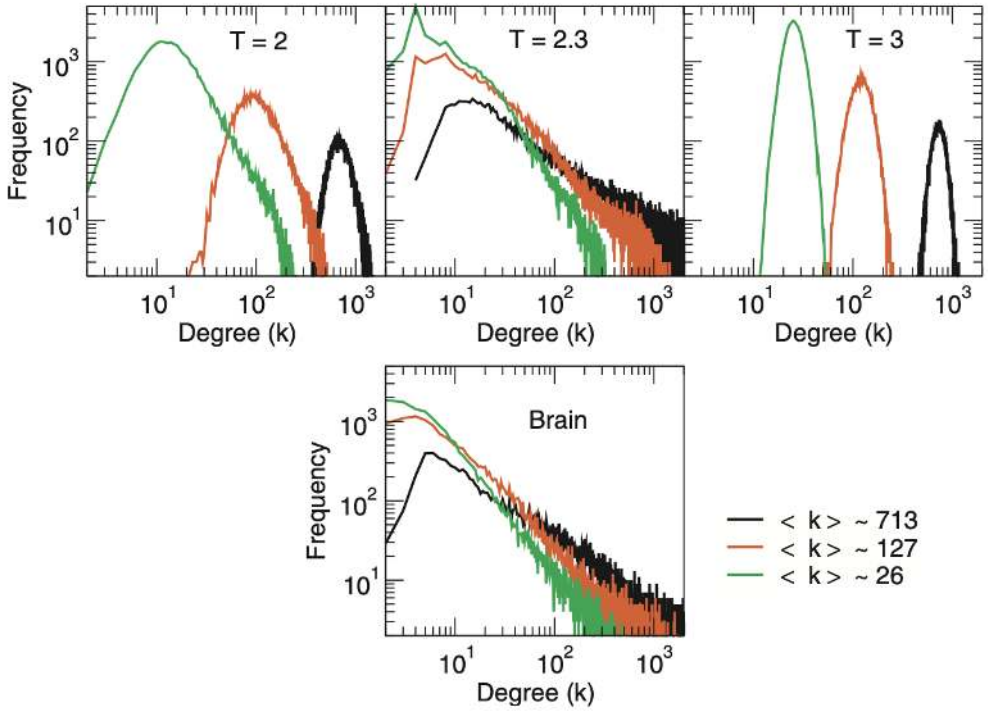

Figure 4.13: Correlation networks constructed by simulating Ising model have the most similarty with connectome's degree distribution at critical point T_c - Graph from [Fraiman et al., 2009]

$$\begin{cases} Q \to E & \text{if } \sum_j W_{ij} s_j(t) > T \\ E \to R & \text{with probability 1} \\ R \to Q & \text{with probability } r_2 \end{cases} \tag{4.7}$$

By tuning the threshold, we observe a transition from sub-critical (where activity quickly dies out) to supercritical (where activity spreads uncontrollably) behavior. This critical behaviour fall into percolation universality class where the second largest cluster shows a pick at the transition point. In percolation theory, the size of the second-largest cluster in a network reflects its ability to transmit information effectively, particularly when facing random failures or disruptions. A larger second-largest cluster signifies higher network resilience and redundancy, which is crucial

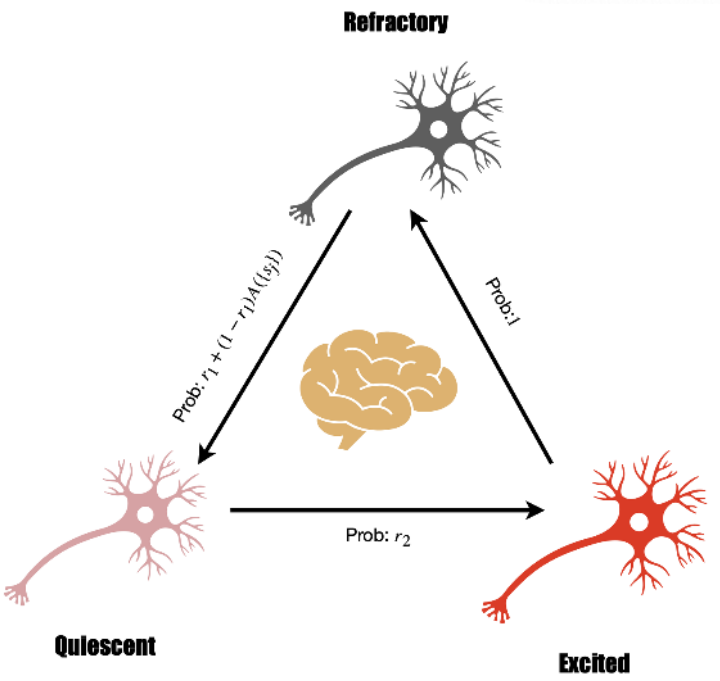

Figure 4.14: Transition circle of a neuron in GH model

for maintaining connectivity and information flow in real-world networks(Fig 6). At the critical point, there is a balance where activity spreads but doesn't take over the entire system, leading to the emergence of scale-invariant patterns. [Haimovici et al., 2013]

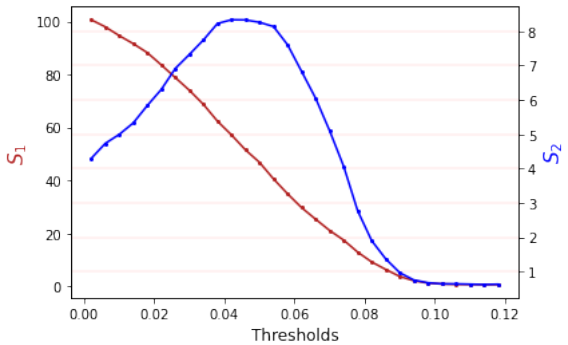

Figure 4.15: Criticality of G-H on Connectome

4.9 Empirical validations of GH dynamics

The GH model significantly simplifies the intricate degrees of freedom inherent in neurophysiological processes. Despite this simplification, its attractiveness lies in its ability to mimic certain experimental results observed in human fMRI data when it is precisely tuned to its critical point. This comparison can be approached from two different angles: either by transforming fMRI experimental time series data into binary states similar to states or by converting simulated data to produce BOLD-like signals.[Haimovici et al., 2013] The extraction of Blood Oxygen Level Dependent (BOLD) signals from fMRI experiments enables us to analyze the behavior of resting state networks (RSNs) within the human brain. By capturing fluctuations in oxygen levels associated with neural activity, BOLD signals provide a window into the functional connectivity and dynamics of RSNs.

Using these BOLD signals, it is possible to compare the behavior of RSNs in humans with those generated by computational models, such as the GH model. In particular, the GH model can be evaluated for its ability to replicate the spatial and temporal characteristics of RSNs observed in empirical fMRI data in different thresholds. For example, the model can be assessed for its accuracy in reproducing the spatial distribution of RSNs. Figure 4.16 shows the comparison of correlation length calculations between functional networks coming from GH model and those of experimental ones. When the model is tuned to Tc, the correlation function for each RSN shows a significant correlation with the experimental. Additionally, the spatial distribution of excited regions aligns well with the experimental data at critical point of model(Figure4.17).

4.9.1 Neural Avalanches of the Greenberg-Hasting model

As discussed in section 4.7.1 avalanches are defined based on the network's activity crossing a set threshold. In Greenberg-Hastings model, the threshold is set to the median of network activity to distinguish significant events from the continuously active network. This thresholding process, although somewhat artificial, is necessary when dealing with empirical data to identify local binary events.The simulations over

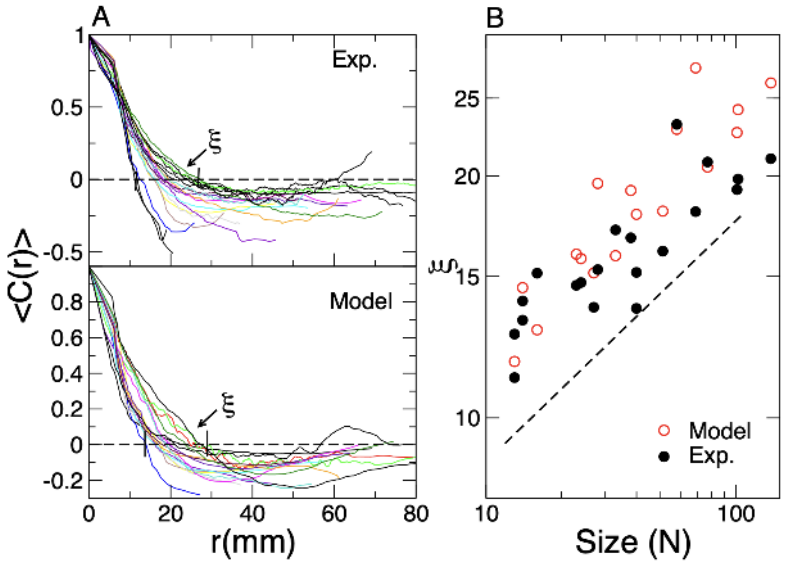

Figure 4.16: Correlation lengths computed for GH model at critical point matches the experimental data

the human connectome show that avalanche sizes follow a nearly linear trend in a log-log scale for small sizes, ending in an exponential truncation for larger sizes. The steepness of the power-law trend is directly related to the threshold, with higher thresholds making it harder for the system to sustain extensive and long-lasting avalanches. These results, however, show a divergence from the expected power-law exponents, making avalanches less relevant for investigating criticality in the GH model compared to other indicators.

To address the limitations of traditional avalanche definitions, the concept of causal avalanches is introduced in [Barzon, 2021]. This approach identifies each spontaneous activation as the start of a new avalanche, which then expands by inducing activation in neighboring nodes.

This method does not require an artificial threshold to mark the end of an event. It can also be defined as the avalanches of single starting nodes in absences of stochasticity. The resulting distributions of avalanche lifetimes and sizes follow a power-law trend, which is robust across different control parameters and closer to experimental observation.

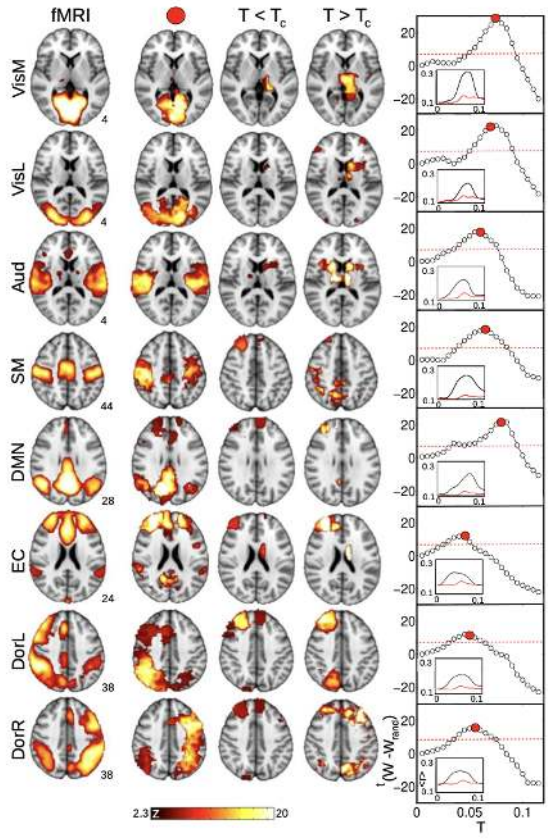

Figure 4.17: The brain's RSN (left column) spontaneously emerges in the model when it is tuned to critical Tc From[Haimovici et al., 2013].

4.9.2 Mean field approach to the model

The mean-field approximation is a foundational analytical method used to simplify complex problems characterized by discrete dynamics. By re-parameterizing the problem, we can express the transition rules as follows:

$$\begin{aligned} U_i(0 \to 1) &= \mu_1 + \alpha\Theta\left(\sum_{j=1}^{N} w_{ij}\epsilon_j\delta(x_j(t),1) - T\right), \\ U_i(1 \to 2) &= \mu_3, \\ U_i(2 \to 0) &= \mu_2. \end{aligned} \tag{4.8}$$

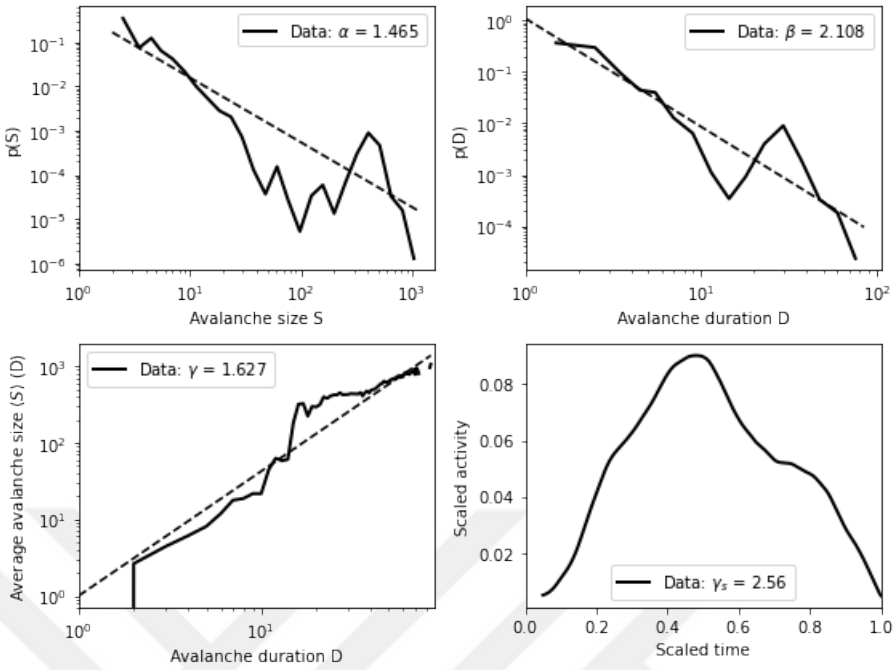

Figure 4.18: Avalanche Analysis of GH Model at critical point

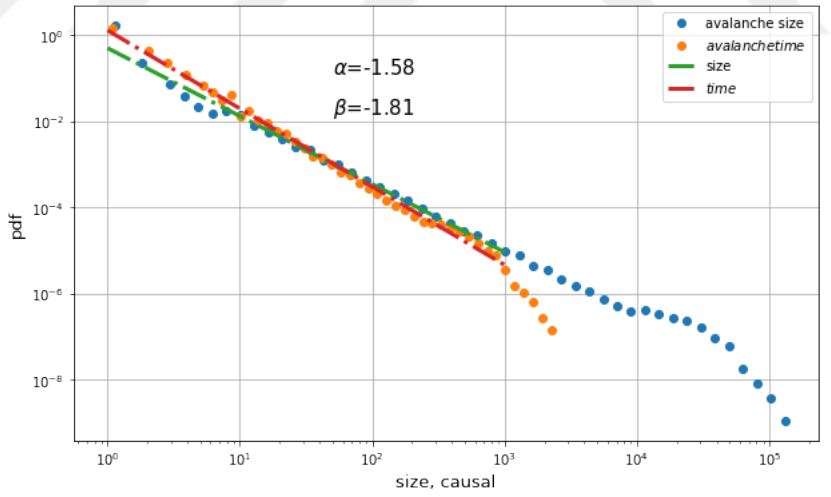

Figure 4.19: Causal Avalanche's Power-law Fit- Exponents agree with experiments

In the mean-field approach, we assume the underlying graph is fully connected with normalized constant weights:

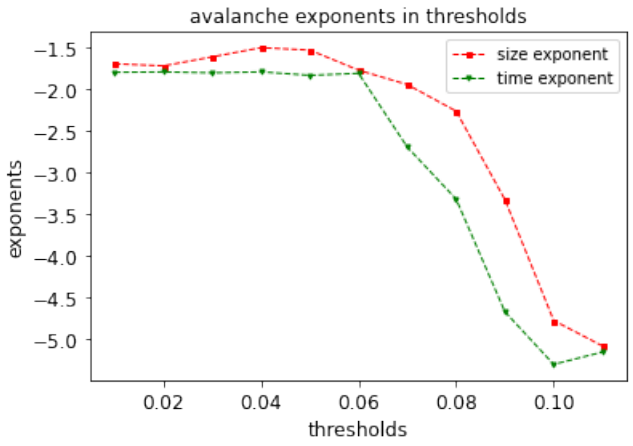

Figure 4.20: Causal Avalanche's exponent behaviour in a range of thresholds

$$W_{ij} = \frac{1}{N}, \quad \forall i, j.$$

This assumption allows us to reduce the problem's complexity by introducing the densities of excited, refractory, and quiescent states, denoted as n_E, n_R, and n_Q, respectively. Utilizing the local transition probabilities from the main text), we can compute the transition probabilities for the populations $\vec{\boldsymbol{n}} = (n_q, n_e, n_r)$:

$$\begin{aligned} U\left(\{n_q, n_e\} \to \{n_q - 1, n_e + 1\}\right) &= \sum_{q \text{ state}} \left(\mu_1 + \alpha\Theta\right) \approx n_q \left(\mu_1 + \alpha\langle\Theta\rangle\right), \\ U\left(\{n_e, n_r\} \to \{n_e - 1, n_r + 1\}\right) &= \sum_{e \text{ state}} \mu_3 = n_e\mu_3, \\ U\left(\{n_r, n_q\} \to \{n_r - 1, n_q + 1\}\right) &= \sum_{r \text{ state}} \mu_2 = n_r\mu_2. \end{aligned} \tag{4.9}$$

Here, $\langle\Theta\rangle$ is defined as:

$$\langle\Theta\rangle \equiv \left\langle \Theta\left(\sum_{j=1}^{N} w_{ij}\delta(x_j(t), 1) - T\right)\right\rangle. \tag{4.10}$$

The approximation made in the first equation, $\Theta \to \langle\Theta\rangle$, is generally valid for a mean-field system. This simplification allows us to handle the dynamics more tractably, providing valuable insights into the behavior of GH dynamics.

4.9.3 Generalization of the mean field approach

The model follows a parallel dynamics in a discrete time t, where the transition probabilities for the i-th site are given by

$$\begin{aligned} P_i(0 \to 1) &= 1 - (1 - r_1)\, A\left(\{x_j\}\right) \\ P_i(1 \to 2) &= 1 \\ P_i(2 \to 0) &= r_2. \end{aligned} \tag{4.11}$$

r_1 is the probability of spontaneous activation, r_2 is related to the average refractory period (with an average duration of 1/r2), and the activation function $A(\{x_j\})$is given by Where

$$A = \left[1 - \Theta\left(\sum_{j \in \Omega_i} W_{ij} \epsilon_j \delta\left(x_j, 1\right) - T\right)\right] \tag{4.12}$$

where Θ is the Heaviside function and $\delta(x, y)$ is the Kroenecker delta function. W_{ij} is a symmetric synaptic matrix, Ω_i is the set of nearest neighbours of the node i and T is the activation threshold, uniform applied on all neurons. The non-null synaptic weights (given by the adjacency matrix of a Watts-Strogatz network) were quenched random variables with an exponential distribution

$$P(W_{ij} = w) = \lambda e^{-\lambda w_{ij}}$$

Assuming that the Heaviside argument behaves as a Gaussian variable we can calculate the average

$$\begin{aligned} \langle \Theta \rangle &= \frac{1}{\sigma\sqrt{2\pi}} \int_{-\infty}^{\infty} \Theta\left(v_i\right) e^{-\frac{(v_i - \mu)^2}{2\sigma^2}}\, \mathrm{d}v_i \\ &= \frac{1}{2}\left[1 + \operatorname{erf}\left(\frac{\mu}{\sqrt{2}\sigma}\right)\right] \equiv \eta(\mu/\sigma) \end{aligned}$$

where $\sigma^2 = \operatorname{Var}\left(v_i\right)$ and

$$\begin{aligned} \mu = \langle v_i \rangle &= \left\langle \sum_{j=1}^{N} w_{ij} \delta\left(x_j(t), 1\right) - T \right\rangle \\ &\approx \frac{\omega}{N} \left\langle \sum_{j \in \text{ exc}}^{N_{\text{exc}}} \delta\left(x_j(t), 1\right) \right\rangle - T \\ &\approx \omega \rho_e - T \end{aligned}$$

where

$$\omega \equiv \langle W_{ij} \rangle .$$

From Eq.(3), wc get $\omega = 1/\beta$. We have also assumed that

$$\langle w_{ij} \delta \left(x_j(t), 1 \right) \rangle \approx \langle w_{ij} \rangle \langle \delta \left(x_j(t), 1 \right) \rangle$$

in a better approximation we can take into account the structure by :

$$\mu_i = \omega_i \rho_e - T \tag{4.13}$$

Where w_i is weighted degree of node i. Thus we can write the activation function specifically for node i :

$$\begin{aligned} \langle \Theta \rangle_i &= \frac{1}{\sigma\sqrt{2\pi}} \int_{-\infty}^{\infty} \Theta \left(v_i \right) e^{-\frac{(v_i - \mu)^2}{2\sigma^2}} \, \mathrm{d}v_i \\ &= \frac{1}{2} \left[1 + \mathrm{erf} \left(\frac{\mu_i}{\sqrt{2}\sigma} \right) \right] \equiv \eta(\mu_i/\sigma) \end{aligned}$$

Where η by the simplified form

$$\eta(x) = \frac{e^{2x}}{1 + e^2 x} \tag{4.14}$$

4.9.4 Analytical appraoch to correlations in GH model

$$\xi_{ij} = \langle \Theta_i \Theta_j \rangle + \langle \Theta \rangle_i \langle \Theta \rangle_j = \alpha \eta(\mu_i/\sigma) \eta(\mu_j/\sigma) + \beta$$

4.9.5 Langevin Equation of GH Model

The transition rates can be expressed in form of a master equation

$$\begin{aligned} \frac{\partial}{\partial t} P(\overrightarrow{\boldsymbol{n}}, t) = & \mu_3 \left(n_e + 1 \right) P \left(n_q, n_e + 1, n_r - 1, t \right) \\ & + \mu_2 \left(n_r + 1 \right) P \left(n_q - 1, n_e, n_r + 1, t \right) \\ & + \left(\mu_1 + \alpha \langle \Theta \rangle \right) \left(n_q + 1 \right) P \left(n_q + 1, n_e - 1, n_r, t \right) \\ & - \left(\mu_3 n_e + \mu_2 n_r + \left(\mu_1 + \alpha \langle \Theta \rangle \right) n_q P(\overrightarrow{\boldsymbol{n}}, t) \right) . \end{aligned} \tag{4.15}$$

By taking the continuum limit of the master equation and an approximation of infinite system($N \to \infty$), we can calculate Taylor expansions up to second order

and ignore higher orders, we can find Kramers-Moyal coefficients of GH model and write the Fokker-Planck equation for the densities $\overrightarrow{\boldsymbol{\rho}} = \overrightarrow{\boldsymbol{n}}/N$ can be derived as

$$\frac{\partial}{\partial t}P(\overrightarrow{\boldsymbol{\rho}},t) = -\sum_i \frac{\partial}{\partial \rho_i}\left[a_i P(\overrightarrow{\boldsymbol{\rho}},t)\right] + \frac{1}{2}\sum_{ij}\frac{\partial^2}{\partial\rho_i\partial\rho_j}\left[b_{ij}P(\overrightarrow{\boldsymbol{\rho}},t)\right] \tag{4.16}$$

Averging over noise we obtain :

$$\begin{aligned}
\dot{\rho_q} &= \mu_2\rho_r - (\mu_1 + \alpha\langle\Theta\rangle)\,\rho_q \\
\dot{\rho_e} &= (\mu_1 + \alpha\langle\Theta\rangle)\,\rho_q - \mu_3\rho_e \\
\dot{\rho_r} &= \mu_3\rho_e - \mu_2\rho_r
\end{aligned} \tag{4.17}$$

Considering the fact that all densities add up to one, we can remove Quiescent state's from the system expression.

$$\begin{aligned}
\dot{\rho_e} &= (1 - f - \rho_e - \rho_r)\,(\mu_1 + \alpha\langle\Theta\rangle) - \mu_3\rho_e \\
\dot{\rho_r} &= \mu_3\rho_e - \mu_2\rho_r
\end{aligned} \tag{4.18}$$

Stationary Solutions:

Equations are restricted to the interval $\left(\rho_e^{\min}, \rho_e^{\max}\right)$, where the limiting values are determined by $\eta(.) = 0$ and $\eta(.) = 1$, respectively. These limiting values are given by:

$$\rho_e^{\min} = \frac{\mu_1\mu_2}{S}$$

and

$$\rho_e^{\max} = \frac{\mu_2\,(1+\mu_1)}{S + \mu_2 + \mu_3},$$

where $S = \mu_1\mu_2 + \mu_2\mu_3 + \mu_3\mu_1$. These values are notably independent of σ.

To delve deeper into the behavior of the system, we assume $r_1 \ll 1$. Under this assumption, we can approximate the minimum density of excited states as:

$$\rho_e^{\min} = \frac{r_1 r_2}{r_1 + r_2 + r_1 r_2} \approx \frac{r_1 r_2}{r_1 + r_2} \approx \frac{r_1 r_2}{r_2} = r_1.$$

This approximation indicates that the minimum activity level corresponds primarily to spontaneous activation events.

Similarly, we can derive the maximum density of excited states as follows:

$$\rho_e^{\max} = \frac{r_2}{2r_2 + 1} = \left(2 + \frac{1}{r_2}\right)^{-1}.$$

This expression shows that the maximum activity level is influenced by the parameter r_2.

In summary, the interval $\left(\rho_e^{\min}, \rho_e^{\max}\right)$ defines the bounds within which the system's activity levels fluctuate. The minimum activity level is largely driven by spontaneous activation (r_1), while the maximum level is determined by the system's intrinsic parameters and their interactions. This analytical framework provides a clear understanding of the stationary solutions in terms of the system's parameters, offering valuable insights into the behavior of complex dynamical systems. Numerical solutions of this approach are presented in [Almeira et al., 2023, Barzon, 2021]. As shown in Figure [FIG], the power spectrum of the model exhibits a peak at the critical threshold T_c.

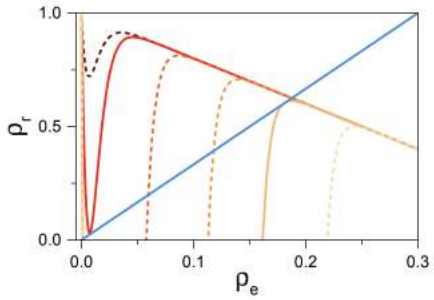

Figure 4.21: Stationary solutions of GH model for different values of T, starting from left, blue line is T=0

Chapter 5

STRUCTURE-FUNCTION INTERPLAY; INSIGHT FROM INFORMATION DIFFUSION

This chapter delves into the intricate relationship between the structural architecture and functional dynamics of complex networks, with a particular focus on the human brain. By exploring the paradigm of information diffusion, we aim to unravel how structural connectivity influences the emergent behaviors and operational efficacy of neural systems. Information diffusion, serving as a proxy for functional interactions, provides a unique lens through which the subtle interdependencies between network topology and dynamic functionality can be examined. Through a combination of theoretical models and empirical data, this analysis seeks to elucidate the critical mechanisms by which structural configurations govern the flow and processing of information, ultimately shaping the cognitive capabilities and resilience of the brain.

5.1 Functional Robustness in Face of Neural Disruptions

5.1.1 criticality under degree preserving edge rewiring

In Chapter One, the process of degree-preserving edge rewiring and its impact on the main characteristics of neural networks were examined. This method was utilized to explore how small-world properties of brain networks deteriorate under randomized perturbations. Specifically, metrics such as clustering coefficient and path length were tracked, revealing a gradual erosion of these key small-world features.
Subsequent simulations implementing Greenberg-Hastings dynamics on an ensemble of perturbed Connectomes highlighted a significant shift in the brain's critical behaviour. The graph in Figure X illustrates the impact of degree-preserving edge rewiring on the critical behavior of neural networks. As indicated, the brain network

exhibits distinct critical behavior compared to its randomized counterparts, which is quantified through the size of the second largest cluster size. The curves demonstrate

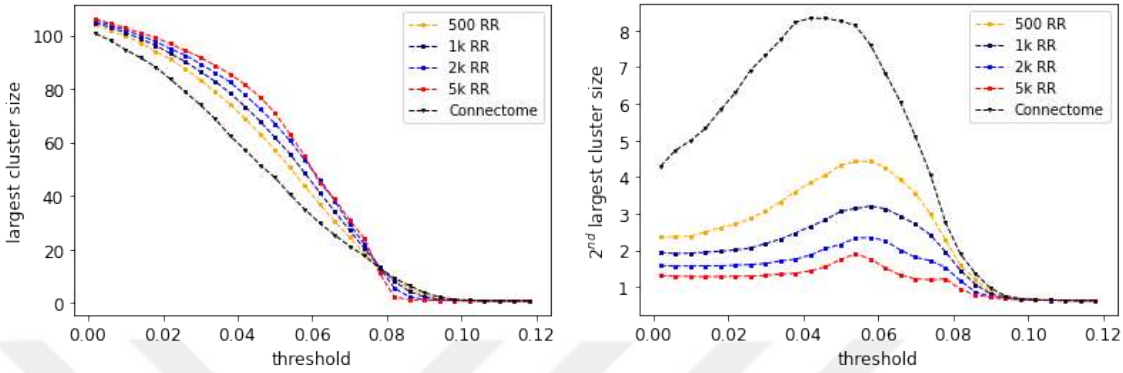

(a) (b)

Figure 5.1: Critical behaviour of randomized brain networks; Each curve represents a different level of randomization: 500, 1000, 2000, and 5000 random rewirings (RR), compared to the original brain network (a) Largest cluster size, (b) second largest cluster size

that as the degree of rewiring increases, the network's peroclation-like critical behavior deviates more noticeably from that of the original brain structure, particularly beyond the 1000 RR threshold. This supports our hypothesis that the small-world nature of brain networks is crucial for maintaining certain functional capabilities, which are compromised when these structural properties are disrupted. The results suggest that even minimal perturbations can lead to significant alterations in network dynamics, underscoring the brain's sensitivity to structural changes. There is a marked decrease in the average size of the second largest connected component of the excited subgraph. In contrast, the size of the largest cluster, which acts as the order parameter in our model, remains relatively unchanged. Furthermore, there is a slight increase in the transition point of the model. This shift could signify an adaptation response within the network's dynamics to maintain functionality amidst structural perturbations.

Although the perturbation of 5-10% of the edges might initially appear minimal, It is crucial to note, , that our analysis is based on a coarse-grained, large-scale

map of the brain comprising only 1,000 nodes (representing voxels). Consequently, a perturbation affecting 10% of these nodes represents a substantial alteration in the context of a real brain, with approximately 86 billion neurons.

The random edge swaps implemented in our degree-preserving rewiring protocol

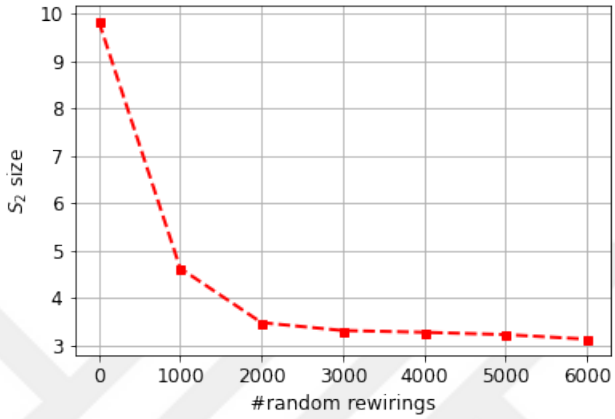

Figure 5.2: Critical behaviour of randomized brain networks

may critically affect the integrity of brain hubs—central nodes that play pivotal roles in neural communication and functional integration. The disruption of these hubs can lead to the degradation of the brain's efficient information processing capabilities, which is explored in next sections employing information theory.

5.1.2 criticality under edge weights shuffling

This randomization technique involves randomly redistributing the weights assigned to the edges in the network while keeping the network topology constant. This analysis helps us in understanding the significance of the role of weight distribution in determining the network's dynamics and functionality. The weights of the edges are randomly reassigned among the edges. This shuffling is done uniformly, where each edge weight is equally likely to be assigned to any edge to maintain the weight distribution. Running G-H dynamics on edge weight randomized connectome seriously affects the critical behaviour of the model and depicts an absorption of second largest cluster size at the critical point.

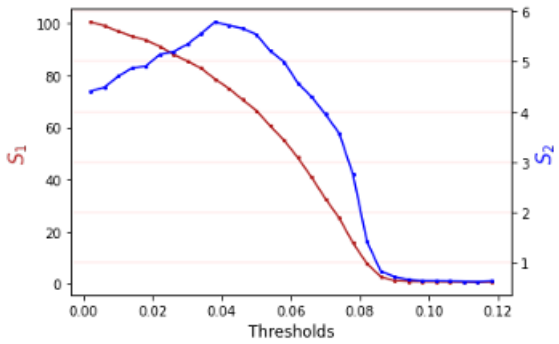

Figure 5.3: Critical behaviour of randomized brain networks

5.1.3 criticality of non-weighted connectome

The critical behavior of a binarized connectome loses the impact of weight distribution, leading to a discontinuous first-order transition into the synchronous phase. This transition point is significantly influenced by the binary cutoff threshold we choose.

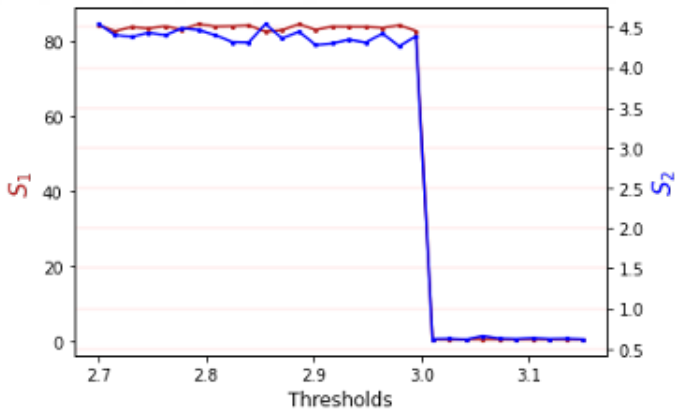

Figure 5.4: Critical behaviour of non weighted human connectome

5.2 Information Theory and Neural Systems

In the seminal 1948 paper [4], Claude Shannon presented a mathematical theory on the concept of information, focusing on its transmission and communication. This

paper introduced a metric capable of measuring a device's information capacity. Expressed in logarithm base 2 units, or bits, this metric indicates the average binary code string length needed to describe a random variable. This concept was named 'Shannon entropy' in his honor.

Shannon's theory, due to its universality and wide applicability, has been influential in various fields related to information transmission and message communication through signals, irrespective of the communication device used.

It's recognized that neurons, serving as transmitters of neural messages, utilize accumulation and release mechanisms as electrical signals. The information capacity of a neuron is assessed based on observed spikes during an experimental time interval, regardless of the potential form. However, the variety of possible states for message transmission from a source and the presence of noise, influenced by various factors like excitement, concentration, or disturbance, complicate the calculation of the information transmission rate. To date, most studies on neuronal information capacity have focused on specific sensory neurons. This is because, unlike brain neurons, sensory neurons receive well-defined input signals, allowing for easier interpretation of each signal emitted by the neuron. An example is the study of a visual sensory neuron responding to a stimulus [5], such as the angular velocity of a wheel generated by a computer." [Shannon, 1948]

5.3 information flow and transfer

Information flow is the transmission of information from one brain region to another. It can be measured using a variety of techniques, including fMRI and EEG. [Shew et al., 2011][Shew et al., 2009] Transfer entropy is a measure of the directed information flow between two time series and is defined as:

$$TE_{Y\to X} = \sum_{x_{t+1},x_t,y_t} p(x_{t+1},x_t,y_t)\log_2\left(\frac{p(x_{t+1}|x_t,y_t)}{p(x_{t+1}|x_t)}\right) \tag{5.1}$$

where:

- $TE_{Y\to X}$ = Transfer entropy from Y to X

- x_t and y_t = the values of time series X and Y at time t
- $p(x_{t+1}, x_t, y_t)$ = the joint probability of X and Y at times t+1, t, and t-1
- $p(x_{t+1}|x_t, y_t)$ = the conditional probability of X at time t+1 given the values of X and Y at times t and t-1
- $p(x_{t+1}|x_t)$ = the conditional probability of X at time t+1 given the value of X at time t.

In our analysis, we have quantified information flow based on the time series analysis of GH dynamics in the brain connectome. Mutual information reveals a peak at the critical point, and its behavior closely mirrors that of the second largest cluster. This suggests a direct relationship between the second largest cluster and the information flow within the brain system.

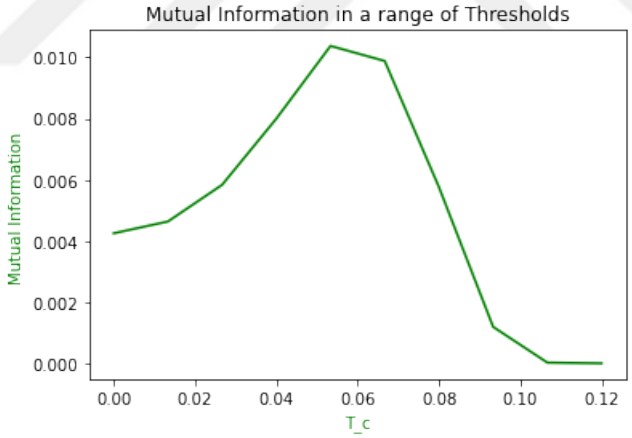

Figure 5.5: Information flow displays a pick at critical point

5.4 Review on brain wiring principles

In the past decades there has been numerous studies on the wiring principles of complex networks [Raj and Chen, 2011, Ying and Wu, 2008, Hagberg and Schult, 2008]. When it comes to brain connectivity, studies often employ simplified models

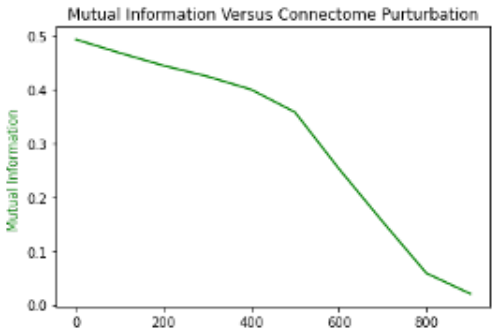

Figure 5.6: Mutual Information flow at critical point decreases rapidly by random rewirings

to uncover fundamental principles. One of the pioneering concepts in this field is the small-world network, introduced by Watts and Strogatz (1998) as discussed in chapter one. They demonstrated that many real-world networks, including neural networks, exhibit properties of both regular and random networks, facilitating efficient information transfer and integration across different brain regions. This small-world organization is optimal for balancing specialized processing and global integration, essential for complex cognitive functions [Watts and Strogatz, 1998]. Building on this foundational work, Gong and van Leeuwen (2004) explored how chaotic neural units evolve into small-world networks through activity-dependent rewiring. They showed that nodes with similar activities form connections while those with differing activities disconnect, resulting in a network structure that is both locally clustered and globally efficient[Gong and van Leeuwen, 2004]. This model underscores the importance of dynamic rewiring in achieving efficient network organization.

Bullmore and Sporns (2009) further extended these concepts by examining the structural and functional dynamics of brain networks. They emphasized the role of modularity, where clusters of highly interconnected nodes (modules) interact with other clusters through a few long-range connections. This modular architecture supports both segregated and integrated processing, crucial for brain function. The brain's ability to adapt these modules through plastic changes in connectivity reflects its capacity for reorganization in response to learning and experience [Bullmore and

Sporns, 2009].

Jarman et al. (2017) employed a heat diffusion model to adaptively rewire a random network, driving it to form small-world structures. They found that increased flow between nodes led to new connections, while decreased flow resulted in disconnections. As the heat kernel's time parameter increased, the network transitioned from modular to more centralized structures, suggesting a critical balance between modularity and centrality [Jarman et al., 2017].

Rubinov et al. (2009) demonstrated how the brain's structural connectivity dynamically changes in response to functional demands through adaptive rewiring mechanisms. Driven by Hebbian plasticity, connections between co-active neurons are strengthened, while those between less active neurons are weakened. This adaptive rewiring ensures the brain maintains efficient information processing capabilities while remaining flexible for new learning experiences [Rubinov et al., 2009].

Graph Laplacian-based methods have also provided significant insights into brain network reorganization. The Laplacian matrix, which measures the difference between a node's value and the average of its neighbors, is used to study diffusion processes in networks. Coifman and Lafon (2006) demonstrated how heat kernel techniques could adaptively rewire networks, promoting efficient and structured connectivity patterns. This approach has been instrumental in understanding how the brain maintains complex connectivity despite continuous dynamic changes [**?**]. In the next sections, we will approach the study of brain architecture through these foundational principles, integrating insights from small-world networks, modular organization, adaptive rewiring, and graph Laplacian methods to uncover the complexity of brain connectivity.

5.5 Information Maximization Rewiring

So far, our observations indicate a strong relationship between information flow within the system and criticality, with both quantities peaking at the critical point. This implies that investigating the brain's structure through the lens of informa-

tion flow among edges could lead to insights into how it achieves high efficiency in entropy transfer across different system levels. A fundamental approach to modeling information diffusion in complex networks is to start with the assumption of linear information diffusion across the graph, analogous to heat diffusion in basic physics. The linear heat diffusion process on a network is essentially about the flow of heat (or information) between connected nodes, influenced by the difference in heat levels between them. For a given node, the heat flow into or out of it depends on its connections (edges to neighbors) and the difference in heat between it and its neighbors.

$$L_{ii}h_i - \sum_{j \in N(i)} A_{ij}h_j = \sum_{j \in N(i)} (h_i - h_j) \tag{5.2}$$

The term $\sum_{j \in N(i)} (h_i - h_j)$ in the discrete setting corresponds to the Laplace operator Δf in continuous domains, where it represents the divergence of the gradient of a function f, indicating how much f at a point is higher or lower than the average of f around that point. For networks, this concept translates into the change in heat (or information) at a node being proportional to the difference between the heat at that node and the average heat of its neighbors, which is exactly what the graph Laplacian computes when applied to the heat vector $h(t)$.

$$\frac{\partial h\,(t)}{\partial t} = -Lh(t) \tag{5.3}$$

the solution to the equation above is :

$$h(t) = e^{-tL} \tag{5.4}$$

which can be written in the eigen basis of Laplacian operator.

$$h(t) = Ve^{-t\Lambda}V^T = \sum_{i=0}^{n-1} e^{-\lambda_i t} v_i v_i^T \tag{5.5}$$

The manner in which diffusion propagates through the graph is governed by the eigenvalue/eigenvector pairs of the Laplacian matrix. The influence of each pair on

the overall diffusion process varies and is contingent upon the size of the eigenvalue. In a connected graph, as t approaches zero, the diffusion behavior can be approximated by $h(t)ILt$, and under these conditions, diffusion is primarily influenced by local connections within the graph.

At 2020, Rentzeperis et al introduced adaptive rewiring based at each step where each node is trying to eliminate the edge with lowest heat(in the context of brain information) transfer and connect to a node with highest transfer. The heats come from eigenvalues of linear graph Laplacian. [Rentzeperis and van Leeuwen, 2020] [Meisel and Gross, 2009]

Information Maximization Algorithm:

The algorithm incorporates a probabilistic component where, with a probability p, rewiring operations are performed at random[Rentzeperis and van Leeuwen, 2020].

Diffusion Rewiring Steps:

1. Initialize by randomized network containing .
2. Randomly select a node, denoted as k, ensuring that k is neither isolated (i.e., it has at least one connection) nor fully connected (i.e., not connected to every other node) with uniform probability.
3. Identify j_1 among all nodes not connected to k as the node with the highest level of heat transfer to k.
4. Determine j_2 among all nodes connected to k as the one with the lowest heat transfer with k.
5. Remove the edge connecting k to j_2 and establish a new edge between k and j_1.

The rate of rewiring, denoted by τ, dictates the duration of the diffusion process before finalizing any rewiring decision. This rate remains fixed throughout the process.

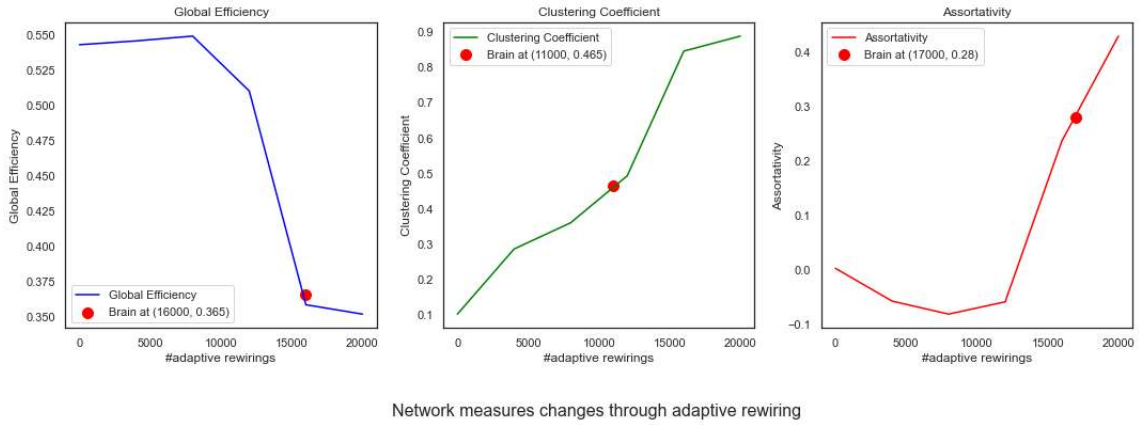

Figure 5.7: adaptive rewiring evolution on randomized brain networks results in brain networks real-space charchtersitcs after approximately 10k rewirings.

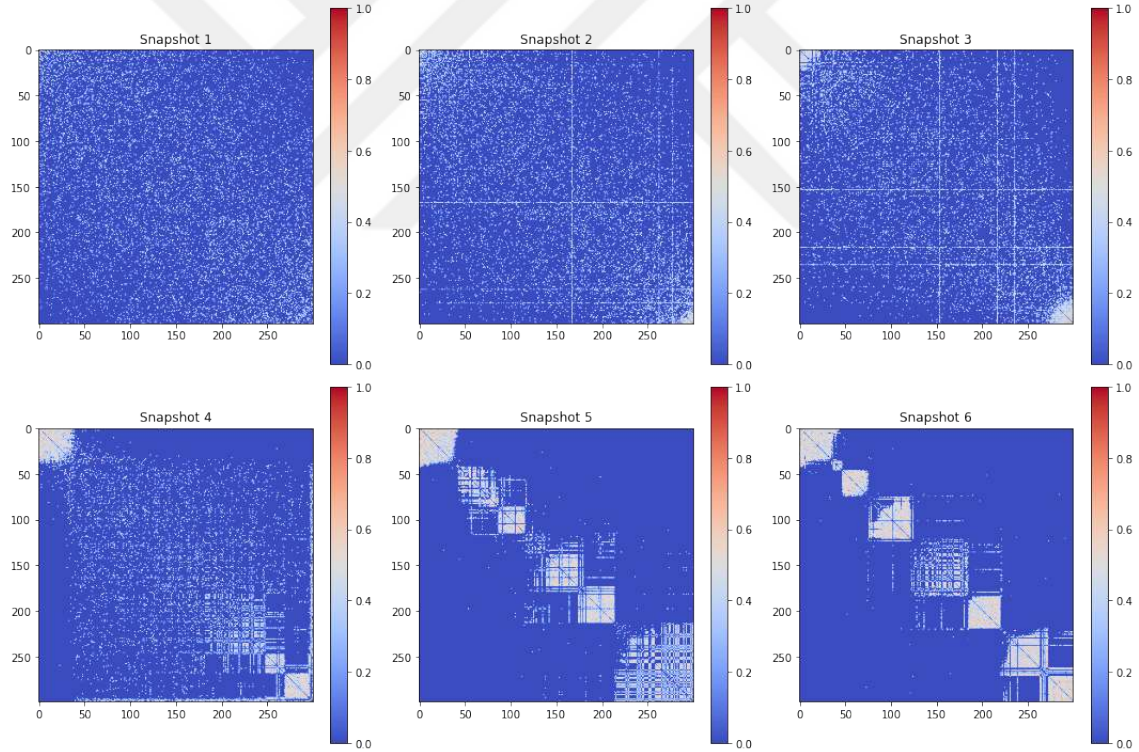

Figure 5.8: Brain-like networks is achieved through information maximization rewirings. Each snapshot is after 5000 adaptive rewires starting from a randomized network.

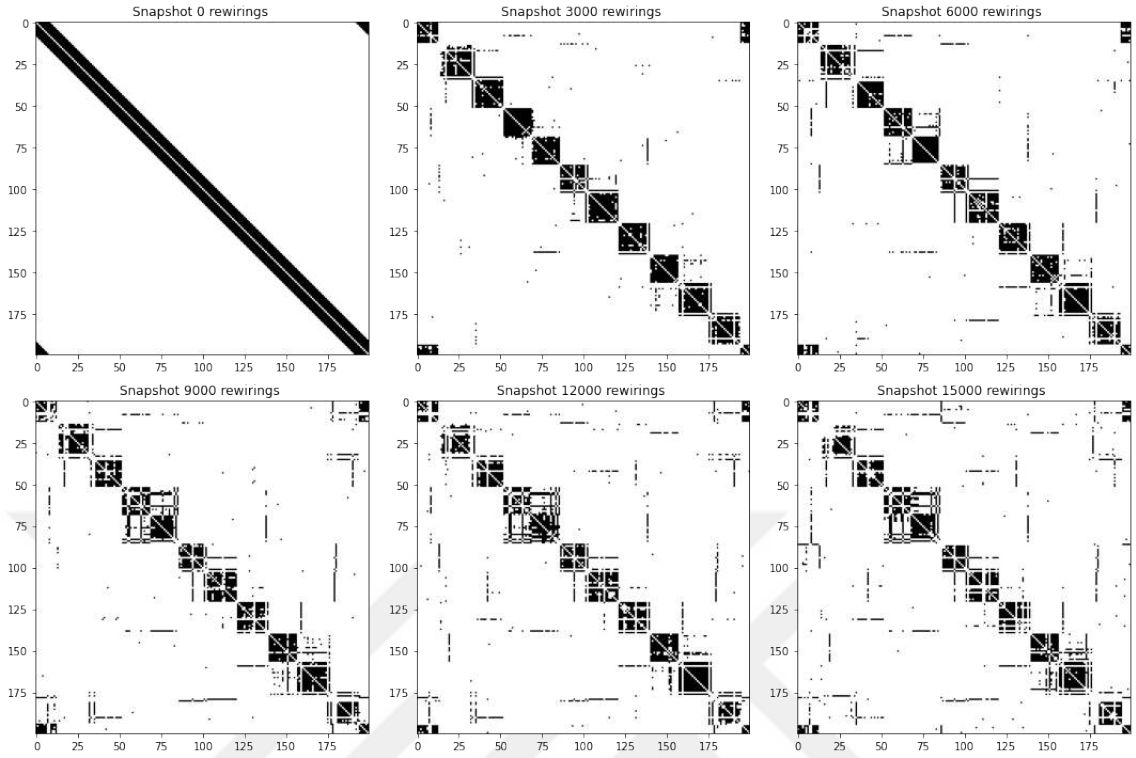

Figure 5.9: Brain-like networks can also be achieved through information maximization rewirings starting from regular graph.(Non-Weighted network)

5.6 Criticality of adaptively rewired networks

After fine optimization of the information maximization algorithm and conducting several experiments, we successfully reconstructed brain networks from randomized brain networks that had lost their critical behavior. By setting the parameter $\tau = 3$ and after approximately 10,000 subsequent rewirings, we achieved the critical state of the brain connectome. Continuing this process led to enhanced criticality, characterized by higher peaks for the second largest cluster, and a reduction in the transition points, as can be seen in Figure 5.9.

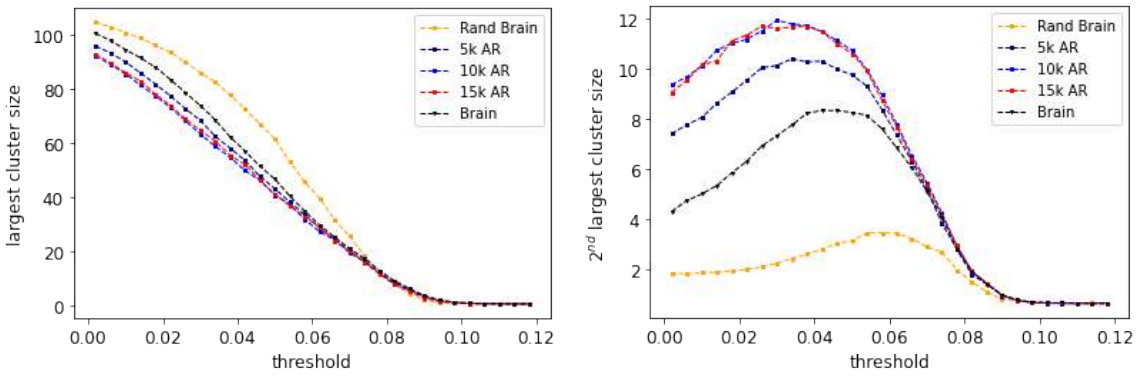

(a) (b)

Figure 5.10: (a) Largest cluster size through adaptive rewirings, (b) second largest cluster size through adaptive rewirings.

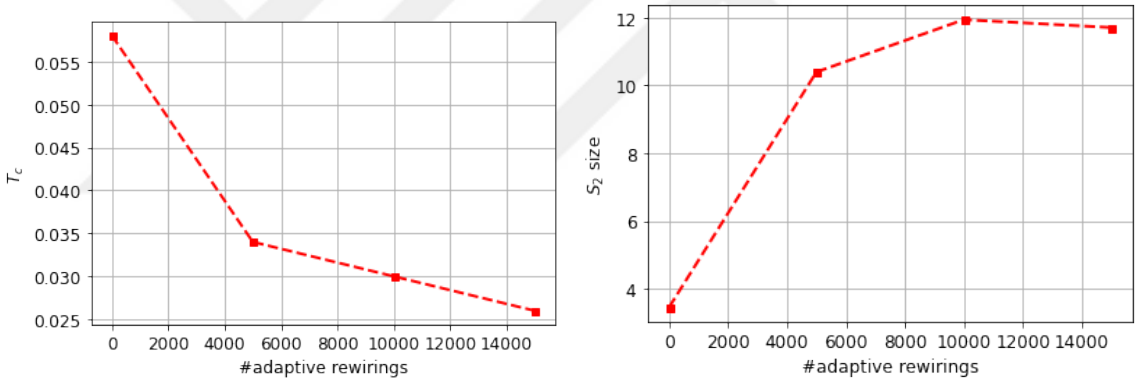

(a) (b)

Figure 5.11: (a) Largest cluster size through adaptive rewirings, (b) second largest cluster size through adaptive rewirings.

5.6.1 How avalanche exponanets change during adaptive rewiring?

5.7 Entropic phase transition of random and adaptively rewired networks

We observe that the Laplacian matrix significantly influences the progression of information from an initial network state, represented as $s(0)$. This state evolves

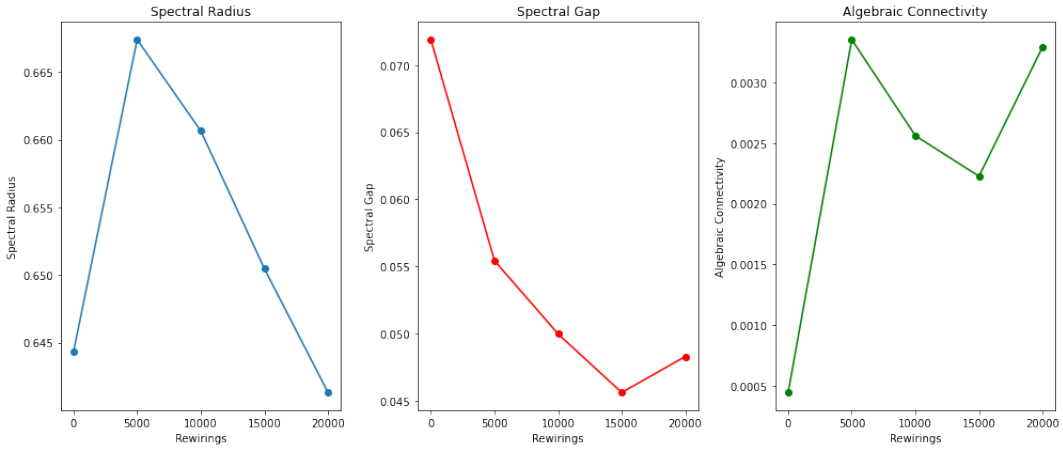

Figure 5.12: Spectral properties of adaptively rewired brain networks .

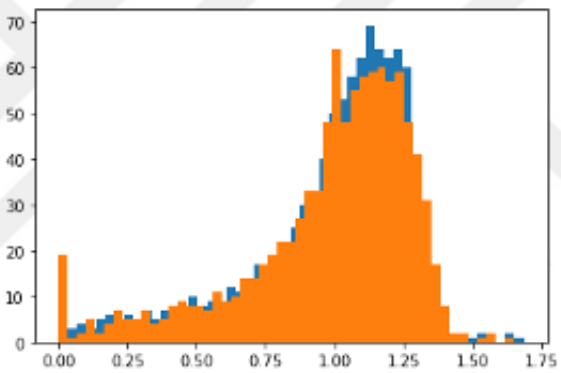

Figure 5.13: Comparison of Laplacian spectrum of 5k adaptively rewired brain connectome and brain connectome. As it can be seen the spectrum remains approximately unchanged.

over time according to the equation:

$$s(\tau) = e^{-\tau \hat{L}} s(0),$$

dictating the dynamics of information flow throughout the network. Villegas et al. defined the network propagator as:

$$\rho(\tau) = \frac{\hat{K}}{\mathrm{Tr}(\hat{K})} = \frac{e^{-\tau \hat{L}}}{\mathrm{Tr}\left(e^{-\tau \hat{L}}\right)} \tag{5.6}$$

The eigenvalues of this propagator are given by:

$$\mu_i(\tau) = \frac{e^{-\lambda_i \tau}}{\sum_j e^{-\lambda_j \tau}} \tag{5.7}$$

nsequently, we can define the Shannon entropy for a network as:

$$S[\rho(\tau)] = -\frac{1}{\log(N)} \sum_{i=1}^{N} \mu_i(\tau) \log \mu_i(\tau) \tag{5.8}$$

Defining the Shannon entropy allows us to consider it as a potential order parameter for the study of entropic phase transitions (or information propagation transitions, i.e., diffusion) over the network. Here phase transition refers to the changes in the entropy of a system that signal a transition from one phase to another, often characterized by a change in the structural order of the system.
Networks undergo a second order phase transition by tuning diffusion time as the tuning parameter τ. [Villegas et al., 2022, Villegas et al., 2023]

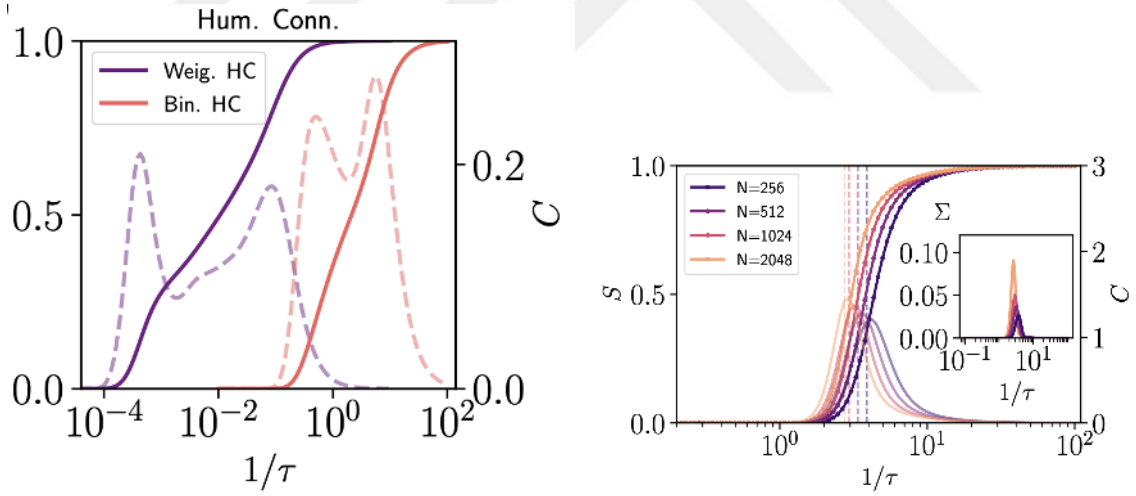

(a) (b)

Figure 5.14: Entropic phase transition of (a)random Erdos rEnyi network (b)human connectome.From[?]

Adaptive rewiring modifies the network's structure, leading to alterations in its Laplacian eigenvalues, which in turn cause a notable increase in Shannon entropy. Below, the relationship between Shannon entropy and the number of adaptive rewiring (AR) events is calculated. It is observed that a phase transition occurs

around the 10k mark, which coincides with the operational level of the brain connectome. Considering the observation that adaptively rewired networks tend to

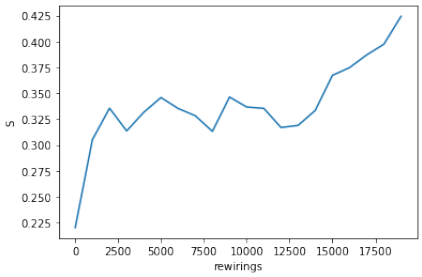

Figure 5.15: adaptive rewiring on random ER network displays an entropic transition

converge to a fixed point in the information maximization procedure, regardless of whether we start from a random network or a regular graph, they become brain-like, modular, and exhibit small-world properties. This suggests that the brain's architecture, characterized by a balance between segregation and integration of structures, is inherently tied to a fixed point in an evolutionary process where feedback loop is entangled with the diffusion of information between neurons.

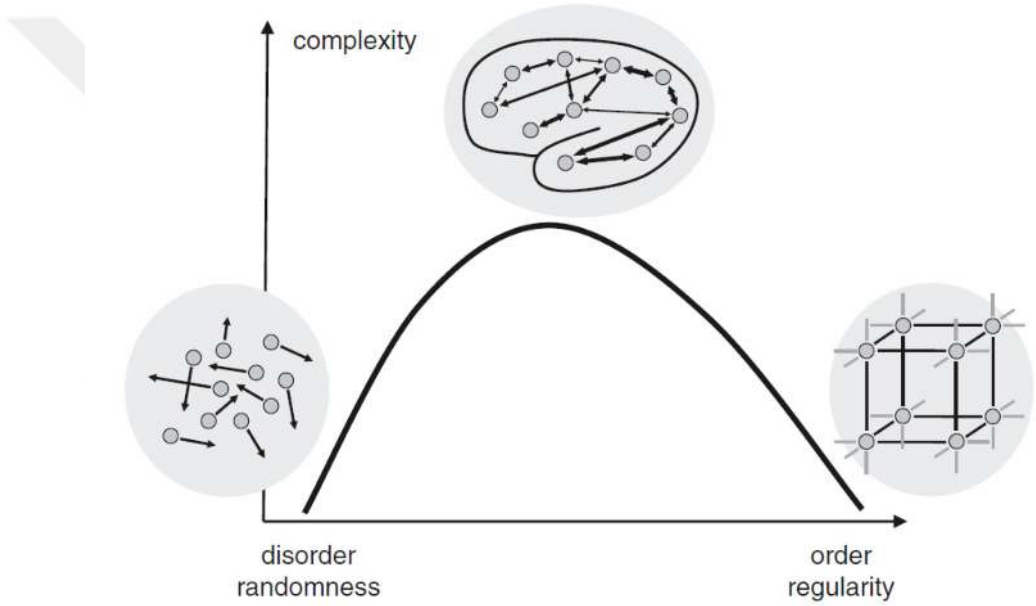

Figure 5.16: structural order determines the functional complexity of brain network- Schematic graph from [Sporns, 2010]

Chapter 6

CONCLUSION

In this thesis, we have explored the profound interconnections between the network architecture and dynamical criticality of the brain, shedding light on how the brain's functional robustness is intricately linked to the structural determinants of its network. Through numerical studies, we have demonstrated that the critical behavior of the brain's network is fundamentally connected to its Laplacian spectrum, unveiling a novel perspective on brain functionality. Our findings suggest that the brain's architectural design is optimized for maximal functional capabilities at the edge of criticality, a state that balances between stability and adaptability.

By employing adaptive rewiring, we reconstructed the brain's architecture, revealing that through entropic phase transitions, the brain network is capable of maximizing its functional abilities. This adaptive process, mimicking evolutionary mechanisms, underscores the brain's remarkable ability to self-organize and adapt to its environment, ensuring efficient information flow and processing.

Furthermore, our analysis has unveiled that the brain operates in a state of self-organized criticality, optimizing information transfer and processing efficiency. This critical state allows the brain to achieve a high level of computational power and adaptability, necessary for its complex functions. The insights gained from the Laplacian spectrum and adaptive rewiring offer a new understanding of the brain's structural and functional coherence, highlighting the intricate balance between the network's architecture and its dynamical states.

Our work contributes to the broader understanding of complex systems, providing a framework for studying other complex networks in nature. By unraveling the interplay between structure and dynamics in the brain, we offer new avenues for research in neuroscience, with potential applications in developing more efficient artificial neural networks in addition to enhancing our understanding of neurologi-

cal disorders. Laplacian-based structural measures may be useful in diagnosing the health and pathology of brains due to their ability to capture essential properties of network connectivity and organization. In conclusion, this thesis underscores the significance of network architecture in determining the brain's functional robustness and critical behavior. The adaptive rewiring and entropic phase transitions observed in the brain network not only highlight the evolutionary advantages of such configurations but also provide a basis for further exploration of criticality in complex systems. As we continue to unravel the mysteries of the brain, the insights gained from this work will contribute to the advancement of neuroscience, offering new perspectives on the fundamental principles governing brain functionality and its remarkable computational abilities.

BIBLIOGRAPHY

[lib,] Complex systems in a nutshell. Math LibreTexts.

[Adriaanse et al., 2014] Adriaanse, S. M., Binnewijzend, M. A., Ossenkoppele, R., Tijms, B. M., van der Flier, W. M., Koene, T., Smits, L. L., Wink, A. M., Scheltens, P., van Berckel, B. N., et al. (2014). Widespread disruption of functional brain organization in early-onset alzheimer's disease. *PLOS ONE*, 9(7):1–12.

[Almeira et al., 2023] Almeira, J., Grigera, T. S., Martin, D. A., Chialvo, D. R., and Cannas, S. A. (2023). Mean-field solution of the neural dynamics in a greenberg-hastings model with excitatory and inhibitory units. *arXiv preprint arXiv:2312.17645*.

[Amit et al., 1985] Amit, D. J., Gutfreund, H., and Sompolinsky, H. (1985). Spin-glass models of neural networks. *Physical Review A*, 32(2):1007.

[Amunts et al., 2019] Amunts, K., Knoll, A. C., Lippert, T., Pennartz, C. M., Ryvlin, P., Destexhe, A., Jirsa, V. K., D'Angelo, E., and Bjaalie, J. G. (2019). The human brain project—synergy between neuroscience, computing, informatics, and brain-inspired technologies. *PLoS biology*, 17(7):e3000344.

[Anderson, 1972] Anderson, P. W. (1972). More is different. *Science*, 177(4047):393–396.

[Author, 2024a] Author, A. (2024a). Emergent phenomena in complex systems: Self-organization, criticality, and spontaneous order. *Journal of Complex Systems*, X:XX–XX.

[Author, 2024b] Author, B. (2024b). Criticality in complex systems: Tipping points and continuous transitions. *Journal of Complexity*, X:XX–XX.

[Author, 2024c] Author, C. (2024c). Structured criticality in complex systems: Small events triggering larger ones. *Journal of Chaos and Complexity*, X:XX–XX.

[Author, 2024d] Author, D. (2024d). Heterogeneity in complex systems: Impact on critical dynamics. *Journal of Adaptive Systems*, X:XX–XX.

[Bak and Paczuski, 1995] Bak, P. and Paczuski, M. (1995). Complexity, contingency, and criticality. *Proceedings of the National Academy of Sciences*, 92(15):6689–6696.

[Barabási, 2016] Barabási, A.-L. (2016). *Network Science*. Cambridge University Press, Cambridge.

[Barzon, 2021] Barzon, G. (2021). Structure-function relation in a stochastic whole-brain model at criticality. Master's thesis, Padova University. Final Dissertation for the Master Degree in Physics of Data.

[Bear, 1995] Bear, M. F. (1995). Mechanism for a sliding synaptic modification threshold. *Neuron*, 15(1):1–4.

[Bear et al., 2020] Bear, M. F., Connors, B. W., and Paradiso, M. A. (2020). *Neuroscience: Exploring the Brain*. Wolters Kluwer, 4 edition.

[Beggs, 2008] Beggs, J. M. (2008). The criticality hypothesis: how local cortical networks might optimize information processing. *Philosophical Transactions of the Royal Society A: Mathematical, Physical and Engineering Sciences*, 366(1864):329–343.

[Beggs and Plenz, 2003] Beggs, J. M. and Plenz, D. (2003). Neuronal avalanches in neocortical circuits. *Journal of neuroscience*, 23(35):11167–11177.

[Bullmore and Sporns, 2009] Bullmore, E. and Sporns, O. (2009). Complex brain networks: graph theoretical analysis of structural and functional systems. *Nature Reviews Neuroscience*, 10(3):186–198.

[Bullmore and Sporns, 2012] Bullmore, E. and Sporns, O. (2012). The economy of brain network organization. *Nature Reviews Neuroscience*, 13(5):336–349.

[Buzsáki, 2006] Buzsáki, G. (2006). *Rhythms of the Brain*. Oxford University Press.

[Castellano et al., 2007] Castellano, C., Castellano, C., and Fortunato, S. e. a. (2007). Statistical physics of social dynamics. *Reviews of Modern Physics*.

[Chialvo, 2004] Chialvo, D. R. (2004). Critical brain networks. *Physica A: Statistical Mechanics and its Applications*, 340(4):756–765.

[Cocchi et al., 2017] Cocchi, L., Gollo, L. L., Zalesky, A., and Breakspear, M. (2017). Criticality in the brain: A synthesis of neuroscience and physics. *Nature Reviews Neuroscience*, 18(10):618–628.

[Cook et al., 2019] Cook, S. J., Jarrell, T. A., Brittin, C. A., Wang, Y., Bloniarz, A. E., Yakovlev, M. A., Nguyen, K. C. Q., Tang, L. T.-H., Bayer, E. A., Duerr, J. S., Bülow, H. E., Hobert, O., Hall, D. H., and Emmons, S. W. (2019). Whole-animal connectomes of both caenorhabditis elegans sexes. *Nature*, 571:63–71.

[de Lange et al., 2014] de Lange, S. C., de Reus, M. A., and van den Heuvel, M. P. (2014). The laplacian spectrum of neural networks. *NeuroImage*, 87:531–543.

[Devlin et al., 2021] Devlin, H., Clare, S., and Tracey, I. (2021). What is fmri? *University of Oxford, Medical Science Division*.

[Diep and Desgranges, 2021] Diep, H. T. and Desgranges, G. (2021). Dynamics of the price behavior in stock markets: A statistical physics approach. *Physica A: Statistical Mechanics and its Applications*, 570:125813.

[Ecker et al., 2015] Ecker, C., Bookheimer, S. Y., and Murphy, D. G. (2015). Intrinsic gray-matter connectivity of the brain in adults with autism spectrum disorder. *Proceedings of the National Academy of Sciences*, 112(29):9327–9332.

[Fornito et al., 2015] Fornito, A., Zalesky, A., and Breakspear, M. (2015). The connectomics of brain disorders. *Nature Reviews Neuroscience*, 16(3):159–172.

[Fraiman et al., 2009] Fraiman, D., Balenzuela, P., Foss, J., and Chialvo, D. R. (2009). Ising-like dynamics in large-scale functional brain networks. *Physical Review E*, 79(6):061922.

[Freeman et al., 2000] Freeman, W. J., Holmes, M. D., West, B. J., and Vanhatalo, S. (2000). Scale-free dynamics of electrocorticograms during epileptic seizures. *Journal of Neuroscience*, 20(4):1505–1514.

[Garcia-Algarra et al., 2013] Garcia-Algarra, J., Galeano, J., Pastor, J., Iriondo, J., and Ramasco, J. (2013). Rethinking the logistic approach for population dynamics of mutualistic interactions. *Journal of Theoretical Biology*.

[Gerstner et al., 2014] Gerstner, W., Kistler, W. M., Naud, R., and Paninski, L. (2014). *Neuronal dynamics: From single neurons to networks and models of cognition*. Cambridge University Press.

[Gong and van Leeuwen, 2004] Gong, P. and van Leeuwen, C. (2004). Evolution to a small-world network with chaotic units. *Europhysics Letters*, 67:328–333.

[Goni et al., 2014] Goni, J., van den Heuvel, M. P., Avena-Koenigsberger, A., Velez de Mendizabal, N., Betzel, R. F., Griffa, A., Hagmann, P., Corominas-Murtra, B., Thiran, J.-P., and Sporns, O. (2014). Resting-brain functional connectivity predicted by analytic measures of network communication. *Proceedings of the National Academy of Sciences*, 111(2):833–838.

[Hagberg and Schult, 2008] Hagberg, A. and Schult, D. A. (2008). Rewiring networks for synchronization. *Chaos: An Interdisciplinary Journal of Nonlinear Science*, 18(3):037105.

[Hagmann et al., 2008] Hagmann, P., Cammoun, L., Gigandet, X., Meuli, R.,

Honey, C. J., Wedeen, V. J., and Sporns, O. (2008). Mapping the structural core of human cerebral cortex. *PLoS biology*, 6(7):e159.

[Haimovici et al., 2013] Haimovici, A., Tagliazucchi, E., Balenzuela, P., and Chialvo, D. R. (2013). Brain organization into resting state networks emerges at criticality on a model of the human connectome. *Physical review letters*, 110(17):178101.

[Helbing et al., 2007] Helbing, D., Johansson, A., and Al-Abideen, H. (2007). Crowd turbulence: the physics of crowd disasters.

[Herz and Hopfield, 1995] Herz, A. V. and Hopfield, J. J. (1995). Earthquake dynamics modeled by self-organized critical states. *Physical Review Letters*, 75(6):1222.

[Hesse and Gross, 2014] Hesse, J. and Gross, T. (2014). Self-organized criticality as a fundamental property of neural systems. *Frontiers in Systems Neuroscience*, 8:166.

[Hodgkin and Huxley, 1952] Hodgkin, A. L. and Huxley, A. F. (1952). A quantitative description of membrane current and its application to conduction and excitation in nerve. *The Journal of Physiology*, 117(4):500–544.

[Honey et al., 2009] Honey, C. J., Sporns, O., Cammoun, L., Gigandet, X., Thiran, J.-P., Meuli, R., and Hagmann, P. (2009). Predicting human resting-state functional connectivity from structural connectivity. *Proceedings of the National Academy of Sciences*, 106(6):2035–2040.

[Jarman et al., 2017] Jarman, N., Steur, E., Trengove, C., Tyukin, I. Y., and Van Leeuwen, C. (2017). Self-organisation of small-world networks by adaptive rewiring in response to graph diffusion. *Scientific Reports*, 7(1):13158.

[Johnston and Wu, 1995] Johnston, D. and Wu, S. M.-S. (1995). *Foundations of Cellular Neurophysiology*. MIT Press.

[Kandel et al., 2013] Kandel, E. R., Schwartz, J. H., Jessell, T. M., Siegelbaum, S. A., and Hudspeth, A. J. (2013). *Principles of Neural Science*. McGraw-Hill, 5 edition.

[Kaur et al., 2021] Kaur, Y., Weiss, S., Zhou, C., Fischer, R., and Hildebrandt, A. (2021). Exploring neural signal complexity as a potential link between creative thinking, intelligence, and cognitive control. *Brain Sciences*, 9(4):59.

[Kelso, 1995] Kelso, J. A. S. (1995). *Dynamic Patterns: The Self-Organization of Brain and Behavior*. MIT Press.

[Kitzbichler et al., 2009] Kitzbichler, M. G., Smith, M. L., Christensen, S. R., and Bullmore, E. (2009). Broadband criticality of human brain network synchronization. *PLoS Computational Biology*, 5(3):e1000314.

[Kuramoto and Kuramoto, 1984] Kuramoto, Y. and Kuramoto, Y. (1984). *Chemical turbulence*. Springer.

[Levina et al., 2007] Levina, A., Herrmann, J. M., and Geisel, T. (2007). Dynamical synapses causing self-organized criticality in neural networks. *Nature physics*, 3(12):857–860.

[Lynn and Bassett, 2019] Lynn, C. W. and Bassett, D. S. (2019). The physics of brain network structure, function and control. *Nat Rev Phys*, 1:318–332.

[Malenka and Bear, 2004] Malenka, R. C. and Bear, M. F. (2004). Ltp and ltd: An embarrassment of riches. *Neuron*, 44(1):5–21.

[Marder and Prinz, 2003] Marder, E. and Prinz, A. A. (2003). Homeostatic regulation of neural function. *Annual Review of Neuroscience*, 26:307–323.

[Meisel and Gross, 2009] Meisel, C. and Gross, T. (2009). Adaptive self-organization in a realistic neural network model. *Physical Review E*, 80(6):061917.

[Moran et al., 2019] Moran, J. K., Michail, G., Heinz, A., Keil, J., and Senkowski, D. (2019). Long-range temporal correlations in resting state beta oscillations are reduced in schizophrenia. *Frontiers in Psychiatry*, 10:517.

[Muñoz, 2018] Muñoz, M. (2018). Criticality and dynamical scaling in living systems. *Reviews of Modern Physics*, 90(3):031001.

[Natascha Schaefer, 2017] Natascha Schaefer (2017). The malleable brain: plasticity of neural circuits and behavior - a review from students to students. *Journal of Neurochemistry*, 142:790–811.

[Naziroglu et al., 2015] Naziroglu, M., Braidy, N., and Trang, T. (2015). Functional importance of transient receptor potential (trp) channels in neurological disorders. *Frontiers in Neuroscience*, 9:189.

[Neumann, 1966] Neumann, J. (1966). The theory of self-reproducing automata. *Univ. of Illinois Press google schola*, 2:429–432.

[Newman, 2010] Newman, M. (2010). *Networks: An Introduction*. Oxford University Press, Oxford.

[Nykter et al., 2008] Nykter, M., Price, N. D., Aldana, M., Ramsey, S. A., Kauffman, S. A., Hood, L. E., Yli-Harja, O., and Shmulevich, I. (2008). Gene expression dynamics in the macrophage exhibit criticality. *Proceedings of the National Academy of Sciences*, 105(6):1897–1900.

[of Health, 2014] of Health, N. I. (2014). Brain 2025 report.

[Pascual-Leone et al., 2005] Pascual-Leone, A., Amedi, A., Fregni, F., and Merabet, L. B. (2005). The plastic human brain cortex. *Annual Review of Neuroscience*, 28:377–401.

[Raj and Chen, 2011] Raj, A. and Chen, Y. (2011). The wiring economy principle: Connectivity determines anatomy in the human brain. *PloS ONE*, 6(9):e14832.

[Rentzeperis and van Leeuwen, 2020] Rentzeperis, I. and van Leeuwen, C. (2020). Adaptive rewiring evolves brain-like structure in weighted networks. *Scientific Reports*, 10(1):6075.

[Rubinov et al., 2009] Rubinov, M., Sporns, O., van Leeuwen, C., and Breakspear, M. (2009). Symbiotic relationship between brain structure and dynamics. *BMC Neuroscience*, 10:55.

[Shannon, 1948] Shannon, C. E. (1948). A mathematical theory of communication. *The Bell System Technical Journal*, 27(3):379–423.

[Shew and Plenz, 2013] Shew, W. L. and Plenz, D. (2013). The functional benefits of criticality in the cortex. *The Neuroscientist*, 19(1):88–100.

[Shew et al., 2009] Shew, W. L., Yang, H., Petermann, T., Roy, R., and Plenz, D. (2009). Neuronal avalanches imply maximum dynamic range in cortical networks at criticality. *Journal of neuroscience*, 29(49):15595–15600.

[Shew et al., 2011] Shew, W. L., Yang, H., Yu, S., Roy, R., and Plenz, D. (2011). Information capacity and transmission are maximized in balanced cortical networks with neuronal avalanches. *Journal of neuroscience*, 31(1):55–63.

[Sporns, 2005] Sporns, O. (2005). The human connectome: A structural description of the human brain. *PLOS Computational Biology*, 1(4):e42.

[Sporns, 2010] Sporns, O. (2010). *Networks of the Brain*. MIT Press.

[Sporns, 2012] Sporns, O. (2012). *Discovering the human connectome*. MIT press.

[Stanley, 1971] Stanley, H. E. (1971). *Introduction to Phase Transitions and Critical Phenomena*. Oxford University Press.

[Stassinopoulos and Bak, 1995] Stassinopoulos, D. and Bak, P. (1995). Democratic reinforcement: A principle for brain function. *Physical Review E*, 51(5):5033.

[Steriade, 2001] Steriade, M. (2001). Impact of network activities on neuronal properties in corticothalamic systems. *Journal of Neurophysiology*, 86(1):1–39.

[Stewart and Plenz, 2008] Stewart, C. V. and Plenz, D. (2008). Homeostasis of neuronal avalanches during postnatal cortex development in vitro. *Journal of neuroscience methods*, 169(2):405–416.

[Tkačik et al., 2015] Tkačik, G., Mora, T., Marre, O., Amodei, D., Palmer, S. E., Berry, M. J., and Bialek, W. (2015). Thermodynamics and signatures of criticality in a network of neurons. *Proceedings of the National Academy of Sciences*, 112(37):11508–11513.

[Tononi and Edelman, 1998] Tononi, G. and Edelman, G. M. (1998). Consciousness and complexity. *Science*, 282(5395):1846–1851.

[Turrigiano, 2012] Turrigiano, G. G. (2012). Homeostatic synaptic plasticity: Local and global mechanisms for stabilizing neuronal function. *Cold Spring Harbor Perspectives in Biology*, 4(1):a005736.

[Turrigiano and Nelson, 2004] Turrigiano, G. G. and Nelson, S. B. (2004). The neurobiology of synaptic scaling. *Annual Review of Neuroscience*, 27:481–507.

[Van Essen et al., 2012] Van Essen, D., Ugurbil, K., Auerbach, E., Barch, D., Behrens, T., Bucholz, R., Chang, A., Chen, L., Corbetta, M., Curtiss, S., et al. (2012). The human connectome project: a data acquisition perspective. *Neuroimage*, 62(4):2222–2231.

[Villegas et al., 2022] Villegas, P., Gabrielli, A., Santucci, F., Caldarelli, G., and Gili, T. (2022). Laplacian paths in complex networks: Information core emerges from entropic transitions. *Physical Review Research*, 4(3):033196.

[Villegas et al., 2023] Villegas, P., Gili, T., Caldarelli, G., and Gabrielli, A. (2023). Laplacian renormalization group for heterogeneous networks. *Nature Physics*, 19(3):445–450.

[Villegas et al., 2014] Villegas, P., Moretti, P., and Munoz, M. A. (2014). Frustrated hierarchical synchronization and emergent complexity in the human connectome network. *Scientific reports*, 4(1):5990.

[Wang et al., 2003] Wang, Y., Chakrabarti, D., Wang, C., and Faloutsos, C. (2003). Epidemic spreading in real networks: an eigenvalue viewpoint. In *22nd International Symposium on Reliable Distributed Systems, 2003. Proceedings.*, pages 25–34.

[Watts and Strogatz, 1998] Watts, D. J. and Strogatz, S. H. (1998). Collective dynamics of 'small-world'networks. *nature*, 393(6684):440–442.

[Ying and Wu, 2008] Ying, X. and Wu, X. (2008). Randomizing social networks: a spectrum preserving approach. In *proceedings of the 2008 SIAM International Conference on Data Mining*, pages 739–750. SIAM.

[Zapperi et al., 1995] Zapperi, S., Lauritsen, K. B., and Stanley, H. E. (1995). Self-organized branching processes: mean-field theory for avalanches. *Physical review letters*, 75(22):4071.

[Zare and Grigolini, 2013] Zare, M. and Grigolini, P. (2013). Criticality and avalanches in neural networks. *Chaos, Solitons & Fractals*, 55:80–94.